Kernel Attractor Networks: A Unifying Framework for Memory Modeling

Anonymous Author(s)
Affiliation
Address
email

Abstract

We consider the problem of training a neural network to store a set of patterns with maximal noise robustness. A solution, in terms of optimal weights and state update rules, is derived by training each individual neuron to perform either kernel classification or interpolation with a minimum weight norm. By applying this method to feed-forward and recurrent networks, we derive optimal networks that include, as special cases, many of the hetero- and auto-associative memory models that have been proposed over the past years, such as modern Hopfield networks and Kanerva's sparse distributed memory. We generalize Kanerva's model and demonstrate a simple way to design a kernel attractor network that can store an exponential number of continuous-valued patterns with a finite basin of attraction. The framework of kernel attractor networks offers a simple and intuitive way to understand the storage capacity of previous memory models, and allows for new biological interpretations in terms of dendritic non-linearities and synaptic clustering.

1 Introduction

Although the classical work on attractor neural networks reached its peak in the late 1980's, with the publication of a number of seminal works [e.g., 2, 18, 20, 23], recent years have seen a renewed interest in the topic, motivated by the popularity of the attention mechanism [60], external memory-augmented neural networks [22, 61], as well as a new generation of energy-based attractor networks models, termed modern Hopfield networks (MHNs), capable of vastly increased memory storage [15, 32]. Recent efforts to understand the theoretical foundation of the attention mechanism have, in fact, shown that it can be linked to Hopfield networks [33, 52], but also to Kanerva's sparse distributed memory (SDM) [7, 27], and to the field of kernel machines [58, 63]. The last connection is particularly intriguing, in light of the many theoretical commonalities between neural networks and kernel methods [8, 9, 25, 43, 62]. Overall, these results suggest that a unified view can offer new insights into memory modeling and new tools for leveraging memory in machine learning.

In this work, we aim to clarify some of the overlap between the fields of memory modeling and statistical learning, by integrating and formalizing a set of theoretical connections between Hopfield networks, the SDM, kernel machines, and neuron models with non-linear dendritic processing.

1.1 Our contribution

- We derive a set of normative kernel-based models that describe the general mathematical structure of feed-forward (i.e., hetero-associative) and recurrent (i.e., auto-associative) memory networks that can perform error-free recall of a given set of patterns with maximal robustness to noise.
- We show that the normative models include, as special cases, the classical and modern Hopfield network, as well as the SDM.

Submitted to 36th Conference on Neural Information Processing Systems (NeurIPS 2022). Do not distribute.

- We derive a simple attractor network model for storing an exponential number of continuous-valued patterns with a finite basin of attraction. We discuss its similarity to attention.

Furthermore, we explain how classifiers with non-linear kernels can be interpreted as general forms of neuron models with non-linear dendritic activation functions and synaptic clustering.

1.2 Related work

Our work is primarily related to [7, 32, 33, 52]. While MHNs are extensively analyzed in [32, 33, 52], the approach is energy-based and makes no statements about the relation between MHNs and other memory models or kernel methods; a brief comment mentions some similarity to SVMs, but this is not further explained [52]. The work by [7] focuses on the SDM and its connection to attention. It observes that the classical Hopfield network is a special case of the SDM, but no further generalization is made, and kernel methods are not mentioned. In our work, we place MHNs and the SDM in a broader theoretical context by showing that *both* models are special suboptimal cases of a family of memory networks that can be derived based on a normative kernel-based approach.

2 Background

Consider the following simple model of hetero-associative memory: a single-layer feed-forward network consisting of a single output neuron connected to N_{in} inputs with the weights $\mathbf{w} \in \mathbb{R}^{N_\phi}$. The output $s_{\text{out}} \in \{-1, +1\}$ is given by

$$s_{\text{out}} = \text{sgn}\Big[\mathbf{w}^\top \boldsymbol{\phi}(\mathbf{s}_{\text{in}}) - \theta\Big] \tag{1}$$

where $\mathbf{s}_{\text{in}}$ is the input vector (also called query), θ the threshold, and $\boldsymbol{\phi}$ a function that maps the "raw" input to a N_ϕ-dimensional feature space, where typically $N_\phi \gg N_{\text{in}}$. Suppose that we are given a set of M input-output patterns $\{\boldsymbol{\xi}^\mu_{\text{in}}, \xi^\mu_{\text{out}}\}_{\mu=1}^M$, where each entry ξ is randomly drawn from $\{-1, +1\}$ with sparseness $f := \mathbb{P}(\xi = 1)$. In order for the neuron to memorize each pattern μ with a maximal attractor basin, it needs to find a set of weights so as to generate the output ξ^μ_{out} in response to the input $\boldsymbol{\xi}^\mu_{\text{in}}$ in a manner that maximizes the Euclidean distance between the input and the decision boundary. Using Gardner's formalism [18, 20], this problem can be expressed as

$$\begin{aligned} \arg\max_{\mathbf{w}} \ \kappa \quad \text{s.t.} \quad & \xi^\mu_{\text{out}}\Big(\mathbf{w}^\top \boldsymbol{\phi}(\boldsymbol{\xi}^\mu_{\text{in}}) - \theta\Big) \geq \kappa, \ \forall \mu \\ & \|\mathbf{w}\|_2 = \bar{w} \end{aligned} \tag{2}$$

where $\bar{w} > 0$ is a constant. This is equivalent to solving

$$\min_{\mathbf{w}} \|\mathbf{w}\|_2 \quad \text{s.t.} \quad \xi^\mu_{\text{out}}\Big(\mathbf{w}^\top \boldsymbol{\phi}(\boldsymbol{\xi}^\mu_{\text{in}}) - \theta\Big) \geq 1, \ \forall \mu \tag{3}$$

which can be directly identified as the support vector machine (SVM) problem for separable data [11]. The solution to Eq. 3 can today be found in any textbook on basic machine learning methods, and yields an optimal output that can be formulated in a *feature* and *kernel* representation

$$s_{\text{out}} = \text{sgn}\left[\sum_\mu^M \alpha^\mu \xi^\mu_{\text{out}} \boldsymbol{\phi}(\boldsymbol{\xi}^\mu_{\text{in}})^\top \boldsymbol{\phi}(\mathbf{s}_{\text{in}}) - \theta\right] = \text{sgn}\left[\sum_\mu^M \alpha^\mu \xi^\mu_{\text{out}} K(\boldsymbol{\xi}^\mu_{\text{in}}, \mathbf{s}_{\text{in}}) - \theta\right] \tag{4}$$

where we have used the "kernel-trick" $K(\mathbf{x}_i, \mathbf{x}_j) = \boldsymbol{\phi}(\mathbf{x}_i)^\top \boldsymbol{\phi}(\mathbf{x}_j)$. The solution depends on the Lagrange coefficients $\alpha^\mu \geq 0$, many of which are typically zero. Patterns with $\alpha^\mu > 0$ are called *support vectors*.

2.1 *Hetero*-associative memory as a feed-forward SVM network

We now consider a hetero-associative memory network with an arbitrary number N_{out} of output neurons, whose combined state we denote $\mathbf{s}_{\text{out}}$. In order for the network as a whole to successfully recall memories with maximal noise robustness, we solve Eq. 3 for each neuron independently. As each neuron can have a different classification boundary along with a different set of support vectors, its weights will, in general, be characterized by an independent set of M Lagrange coefficients. To

simplify the notation, we represent these coefficients α_i^μ, across neurons i and patterns μ, as entries in the matrix $\mathbf{A}$, where $(\mathbf{A})_{i\mu} = \alpha_i^\mu$. We also combine all thresholds in the vector $\boldsymbol{\theta} = (\theta_1, \ldots, \theta_{N_{\text{out}}})$, and all input and output patterns as columns in the matrices $\mathbf{X}_{\text{in}} = (\boldsymbol{\xi}_{\text{in}}^1, \ldots, \boldsymbol{\xi}_{\text{in}}^M)$ and $\mathbf{X}_{\text{out}} = (\boldsymbol{\xi}_{\text{out}}^1, \ldots, \boldsymbol{\xi}_{\text{out}}^M)$. Finally, we assume that all neurons have the same feature map, so that $\boldsymbol{\phi}_i = \boldsymbol{\phi}, \forall i$ (see Fig. 1). The optimal response of the network is compactly summarized as follows.

Property 1 (Robust hetero-associative memory)**.** *The optimal output of a single-layer hetero-associative memory network trained to recall the patterns $\mathbf{X}_{\text{out}}$ in response to the inputs $\mathbf{X}_{\text{in}}$, with maximal noise robustness, can be written in the form*

$$\mathbf{s}_{\text{out}} = \text{sgn}\Big[(\mathbf{A} \odot \mathbf{X}_{\text{out}})\boldsymbol{\phi}(\mathbf{X}_{\text{in}})^\top \boldsymbol{\phi}(\mathbf{s}_{\text{in}}) - \boldsymbol{\theta}\Big] \qquad \textit{(feature)} \tag{5}$$

$$= \text{sgn}\big[(\mathbf{A} \odot \mathbf{X}_{\text{out}})K(\mathbf{X}_{\text{in}}, \mathbf{s}_{\text{in}}) - \boldsymbol{\theta}\big] \qquad \textit{(kernel)} \tag{6}$$

where $\odot$ denotes the Hadamard product.

3 Kernel attractor networks for binary patterns

3.1 *Auto*-associative memory as a recurrent SVM network

We begin our results by first noting that the hetero-associative memory network can be made auto-associative by setting $N_{\text{out}} = N_{\text{in}}$ and $\mathbf{X}_{\text{out}} = \mathbf{X}_{\text{in}}$. The network is now effectively recurrent, as each neuron serves both as an input and output simultaneously (see Fig. 1). Consider a recurrent network with N neurons, whose state at time point t is denoted $\mathbf{s}^{(t)} \in \{-1, +1\}^N$, and whose dynamics evolve according to the update rule

$$s_i^{(t+1)} = \text{sgn}\Big[\mathbf{w}_i^\top \boldsymbol{\phi}(\mathbf{s}^{(t)}) - \theta_i\Big] \tag{7}$$

where $\mathbf{w}_i \in \mathbb{R}^{N_\phi}$ is the weight vector to neuron $i = 1, \ldots, N$. In order to make the patterns $\{\boldsymbol{\xi}^\mu\}_{\mu=1}^M$ attractors of the network dynamics, each neuron i is, again, independently trained on every pattern μ to produce the response ξ_i^μ when the rest of the network is initialized in $\boldsymbol{\xi}^\mu$. Moreover, the noise robustness and, thereby, the size of the attractor basins, can be maximized by maximizing the Euclidean distance between each neuron's decision boundary and the patterns [16, 29]. The problem of training the entire network can, in this way, be transformed into the problem of training N separate classifiers according to

$$\min_{\mathbf{w}_i} \|\mathbf{w}_i\|_2 \quad \text{s.t.} \quad \xi_i^\mu \Big(\mathbf{w}_i^\top \boldsymbol{\phi}(\boldsymbol{\xi}^\mu) - \theta_i\Big) \geq 1, \ \forall \mu, i \ . \tag{8}$$

The solution can be obtained by slightly modifying Property 1, and is stated below.

Property 2.1 (Robust auto-associative memory)**.** *A recurrent auto-associative memory network trained to recall the patterns $\mathbf{X}$ with maximal noise robustness has an optimal synchronous update rule that can be written in the form*

$$\mathbf{s}^{(t+1)} = \text{sgn}\Big[(\mathbf{A} \odot \mathbf{X})\boldsymbol{\phi}(\mathbf{X})^\top \boldsymbol{\phi}(\mathbf{s}^{(t)}) - \boldsymbol{\theta}\Big] \qquad \textit{(feature)} \tag{9}$$

$$= \text{sgn}\Big[(\mathbf{A} \odot \mathbf{X})K(\mathbf{X}, \mathbf{s}^{(t)}) - \boldsymbol{\theta}\Big] \qquad \textit{(kernel)} \ . \tag{10}$$

Remark. With a linear feature map $\boldsymbol{\phi}(\mathbf{x}) = \mathbf{x}$, the optimal update is reduced to

$$\mathbf{s}^{(t+1)} = \text{sgn}\Big[\mathbf{W}\mathbf{s}^{(t)} - \boldsymbol{\theta}\Big], \quad \mathbf{W} = (\mathbf{A} \odot \mathbf{X})\mathbf{X}^\top \tag{11}$$

where $\mathbf{W}$ is the general form of the optimal weight matrix.

The solution described by Property 2.1 does not, in general, prohibit a neuron from having self-connections. Applying this constraint yields the following result.

Property 2.2 (Robust auto-associative memory without self-connections)**.** *A recurrent auto-associative memory network without self-connections, that has been trained to recall the patterns $\mathbf{X}$ with maximal noise robustness, has an optimal update rule that can be written in the kernel representation*

$$s_i^{(t+1)} = \text{sgn}\left[\sum_\mu^M \alpha_i^\mu \xi_i^\mu k\left(\sum_{j \neq i}^N \xi_j^\mu s_j^{(t)}\right) - \theta_i\right] \tag{12}$$

where k is an inner-product kernel, i.e. $K(\mathbf{x}_i, \mathbf{x}_j) = k(\mathbf{x}_i^\top \mathbf{x}_j)$.

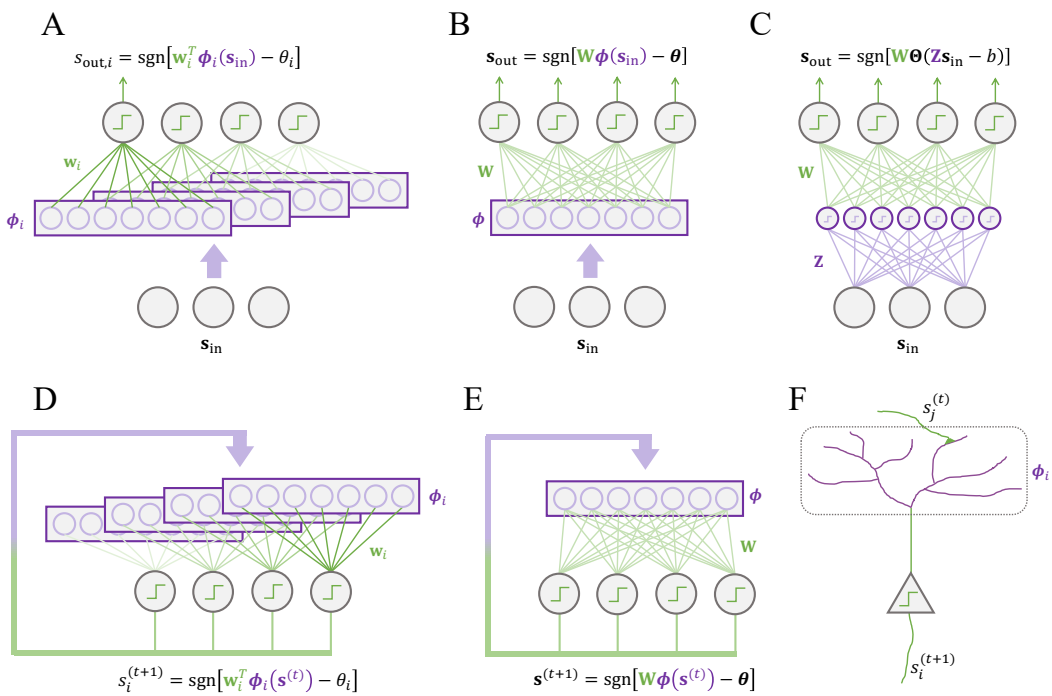

Figure 1: Graphical representation of (A-B) the feed-forward SVM network, (C) the SDM, (D-E) the recurrent SVM network, and (F) an SVM mapped to the anatomy of a pyramidal cell (see Sec. 5). Circles represent neurons, while boxes represent the intermediate transformation of the input by the feature map $\boldsymbol{\phi}$, which can be dependent (A, D) or independent (B, E) of neuron index i.

Remark. When the kernel is linear, i.e. $k(\mathbf{x}_i^\top \mathbf{x}_j) = \mathbf{x}_i^\top \mathbf{x}_j$, the update reduces to

$$s_i^{(t+1)} = \text{sgn}\left[\sum_{\mu}^{M} \alpha_i^\mu \xi_i^\mu \sum_{j \neq i}^{N} \xi_j^\mu s_j^{(t)} - \theta_i\right]. \tag{13}$$

Storage capacity. An intuition for the storage capacity scaling of the hetero- and auto-associative memory network can be gained by observing that the network as a whole will be able to successfully recall patterns as long as each neuron is able to correctly classify its inputs (or is very unlikely to produce an error). The capacity of the network can thereby be derived from the capacity of each individual neuron. It is well-known that a linear binary classifier can learn to correctly discriminate a maximum of $M_{\max} \approx 2D_{\text{VC}}$ random patterns, where D_{VC} is the Vapnik-Chervonenkis dimension of the model [13, 18, 37, ch. 40]. When the neuron in Eq. 7 has a linear feature map $\boldsymbol{\phi}(\mathbf{x}) = \mathbf{x}$, this results in $D_{\text{VC}} = N$ and, thus, the capacity $M_{\max} \approx 2N$. Suppose, on the other hand, that the kernel is a homogeneous polynomial of degree p, so that $K(\mathbf{x}_i, \mathbf{x}_j) = (\mathbf{x}_i^\top \mathbf{x}_j)^p$. In this case, $\boldsymbol{\phi}$ will contain all monomials of degree p composed of the entries in $\mathbf{x}$. As there are $\mathcal{O}(N^p)$ unique p-degree monomials (see Appendix A), the input dimensionality and $M_{\max}$ will be $\mathcal{O}(N^p)$. For the exponential kernel, which we can write as $K(\mathbf{x}_i, \mathbf{x}_j) = \exp(\mathbf{x}_i^\top \mathbf{x}_j) = \sum_{p=0}^{\infty} (\mathbf{x}_i^\top \mathbf{x}_j)^p / p!$, the dimensionality of $\boldsymbol{\phi}$ will be $\sum_{p=0}^{N} \binom{N}{p} = 2^N$, which gives $M_{\max} \sim \mathcal{O}(e^N)$.

Application to special cases. In the following sections, we will show that many of the models of hetero- and auto-associative memory that have been proposed over the past years can be seen as specific cases of the solutions in Properties 1, 2.1, and 2.2, characterized by specific choices of $\mathbf{A}$ and functions $\boldsymbol{\phi}$ and K.

3.2 Kanerva's sparse distributed memory is a feed-forward SVM network

The sparse distributed memory (SDM), developed by Kanerva [27], is one of the most famous examples of a hetero-associative memory model. It has lately received much attention in the context of generative memory models [64] and attention layers in transformers [7].

The SDM consists of a register of N_ϕ memory slots, each associated with an address $\mathbf{z}_i \in \{-1,+1\}^{N_{\text{in}}}$, $i = 1, \ldots, N_\phi$. All addresses are listed as rows in the matrix $\mathbf{Z} = (\mathbf{z}_1, \ldots, \mathbf{z}_{N_\phi})^\top$. The content of each slot is represented by an N_{out}-dimensional vector, initialized at zero. Suppose that we wish to store the M patterns $\mathbf{X}_{\text{out}} = (\boldsymbol{\xi}^1_{\text{out}}, \ldots, \boldsymbol{\xi}^M_{\text{out}})$ in the addresses $\mathbf{X}_{\text{in}} = (\boldsymbol{\xi}^1_{\text{in}}, \ldots, \boldsymbol{\xi}^M_{\text{in}})$, where all entries are random and bipolar. The basic idea of the SDM is to write the data to, and later read it from, multiple memory slots at once (hence the distributed storage); this ensures a degree of noise-robustness. In mathematical terms, the read-out of the SDM provided with a query $\mathbf{s}_{\text{in}}$, is given by

$$\mathbf{s}_{\text{out}} = \text{sgn}\Big[\mathbf{X}_{\text{out}}\, \Theta(\mathbf{Z}\mathbf{X}_{\text{in}} - b)^\top\, \Theta(\mathbf{Z}\mathbf{s}_{\text{in}} - b)\Big] \tag{14}$$

where Θ the Heaviside function with bias $b = N_{\text{in}} - 2r$, and r is a parameter that determines the precision of the writing and reading process. Upon comparing Eqs. 14 and 5, the SDM can be directly identified as a special case of a suboptimal feed-forward SVM network in the feature representation, with $\mathbf{A} = \mathbf{1}$, $\boldsymbol{\theta} = \mathbf{0}$, and the feature map $\boldsymbol{\phi}_{\text{SDM}}(\mathbf{x}) = \Theta(\mathbf{Z}\mathbf{x} - b)$. When viewed as a kernel method, the function of the SDM is to store the dense addresses $\mathbf{X}_{\text{in}}$ as sparse high-dimensional representations $\boldsymbol{\phi}_{\text{SDM}}$, to make it easier to later determine the slots closest to a query $\mathbf{s}_{\text{in}}$, and retrieve the relevant data.

Capacity. As the SDM is linear in $\boldsymbol{\phi}_{\text{SDM}}$, with $D_{\text{VC}} \approx N_\phi$, it follows from the analysis in Sec. 3.1 that one should expect the capacity to scale as $M_{\max} \sim \mathcal{O}(N_\phi)$. Moreover, one should expect a proportionality constant $\sim$0.1, since the SDM is suboptimal relative to the feed-forward SVM network, analogously to how the classical Hopfield network is suboptimal relative to the recurrent SVM network (see Sec. 3.3). This is consistent with earlier proofs [10, 28].

Kernel of an infinite SDM. In practice, an SDM with a large number of memory slots N_ϕ requires calculations involving a large address matrix $\mathbf{Z}$. This can be avoided by applying the kernel-trick in the limit $N_\phi \to \infty$. In this section, we will derive the kernel corresponding to two different variants of the SDM and demonstrate that both are translation-invariant. To ensure convergence, we will define the kernel as

$$K_{\text{SDM}}(\mathbf{x}_i, \mathbf{x}_j) = \lim_{N_\phi \to \infty} \frac{\boldsymbol{\phi}_{\text{SDM}}(\mathbf{x}_i)^\top \boldsymbol{\phi}_{\text{SDM}}(\mathbf{x}_j)}{N_\phi}\ . \tag{15}$$

It is interesting to note here that $\boldsymbol{\phi}_{\text{SDM}}$ is equivalent to a single-layer neural network with N_ϕ neurons, weights $\mathbf{Z}$, and bias b. This means that K_{SDM} is equivalent to the kernel of an infinitely wide neural network [9, 43, 62].

We begin by noticing that $\boldsymbol{\phi}_{\text{SDM}}(\mathbf{x})$ has a geometrical interpretation [7, 28]. It is a binary vector that indicates those memory addresses in $\mathbf{Z}$ that differ by at most r bits compared to $\mathbf{x}$. For any two bipolar vectors $\mathbf{z}$ and $\mathbf{x}$, the bit-wise difference can be computed as $\frac{1}{2}|\mathbf{z} - \mathbf{x}| = \frac{1}{4}\|\mathbf{z} - \mathbf{x}\|_2^2$. This means that $\boldsymbol{\phi}_{\text{SDM}}(\mathbf{x})$ indicates all addresses that lie within a sphere centered at $\mathbf{x}$ with radius $2\sqrt{r}$. Consequently, the inner product $\boldsymbol{\phi}_{\text{SDM}}(\mathbf{x}_i)^\top \boldsymbol{\phi}_{\text{SDM}}(\mathbf{x}_j)$ is the number of addresses located in the overlapping volume of two spheres centered at $\mathbf{x}_i$ and $\mathbf{x}_j$. Although an exact calculation of this quantity can be found in [7, 27], its connection to the SDM kernel has, to the best of our knowledge, not previously been made. We therefore modify the previously published expression with a normalization factor $1/2^{N_{\text{in}}}$ and state the following property.

Property 3.1 (Kernel of an infinite SDM on the hypercube)**.** *In the limit $N_\phi \to \infty$, the read-out of an SDM with N_ϕ memory slots, storing M patterns $\mathbf{X}_{\text{out}}$ in the addresses $\mathbf{X}_{\text{in}}$, is given by*

$$\mathbf{s}_{\text{out}} = \text{sgn}\big[\mathbf{X}_{\text{out}} K_{\text{SDM}}(\mathbf{X}_{\text{in}}, \mathbf{s}_{\text{in}})\big] \tag{16}$$

where

$$K_{\text{SDM}}(\mathbf{x}_i, \mathbf{x}_j) = \frac{1}{2^{N_{\text{in}}}} \sum_{i=N_{\text{in}}-r-\lfloor\frac{\Delta}{2}\rfloor}^{N_{\text{in}}-\Delta} \sum_{j=[N_{\text{in}}-r-i]_+}^{\Delta-(N_{\text{in}}-r-i)} \binom{N_{\text{in}}-\Delta}{i} \cdot \binom{\Delta}{j} \tag{17}$$

and where r is the bit-wise error threshold and Δ is the bit-wise difference between $\mathbf{x}_i$ and $\mathbf{x}_j$, given by $\Delta = \frac{1}{2}|\mathbf{x}_i - \mathbf{x}_j| = \frac{1}{4}\|\mathbf{x}_i - \mathbf{x}_j\|_2^2$.

The SDM can also be implemented with continuous addresses, randomly placed on a unit hypersphere of $(N_{\text{in}} - 1)$ dimensions, denoted $\mathbb{S}^{N_{\text{in}}-1}$. The vector $\boldsymbol{\phi}_{\text{SDM}}(\mathbf{x})$ now indicates all addresses that lie within a hyperspherical cap centered at $\mathbf{x}$ with an angle $\arccos(b)$ between its central axis and the rim. The inner product $\boldsymbol{\phi}_{\text{SDM}}(\mathbf{x}_i)^\top \boldsymbol{\phi}_{\text{SDM}}(\mathbf{x}_j)$ is the number of addresses located in the overlapping area of two spherical caps centered at $\mathbf{x}_i$ and $\mathbf{x}_j$. While a calculation of this quantity, again, can be found in [7], it has not previously been connected to the kernel of an SDM. We simplify the previously published result and also derive a closed-form approximation, valid for highly sparse $\boldsymbol{\phi}_{\text{SDM}}$ (see Appendix B for details). The results are summarized below.

Property 3.2 (Kernel of an infinite SDM on the unit hypersphere)**.** *In the limit $N_\phi \to \infty$, the read-out of an SDM with N_ϕ memory slots, storing M patterns $\mathbf{X}_{\text{out}}$ in the addresses $\boldsymbol{\xi}_{\text{in}}^\mu \in \mathbb{S}^{N_{\text{in}}-1}$, $\forall \mu$, is given by Eq. 16 with the kernel*

$$K_{\text{SDM}}(\mathbf{x}_i, \mathbf{x}_j) = \frac{N_{\text{in}} - 2}{2\pi} \int_{\alpha_x}^{\alpha_b} \sin(\varphi)^{N_{\text{in}}-2} B\left[1 - \frac{\tan^2(\alpha_x)}{\tan^2(\varphi)}; \frac{N_{\text{in}} - 2}{2}, \frac{1}{2}\right] \mathrm{d}\varphi \tag{18}$$

where $\alpha_x = \frac{1}{2}\arccos(\mathbf{x}_i^\top \mathbf{x}_j)$, $\alpha_b = \arccos(b)$, and B is the incomplete Beta function (details in Appendix B.1). In the highly sparse regime, when $0.9 \lesssim b < 1$ and $\frac{1}{N_\phi}\|\boldsymbol{\phi}_{\text{SDM}}\|_0 \ll 1$, the kernel can be approximated with

$$K_{\text{SDM}}(\mathbf{x}_i, \mathbf{x}_j) \approx \frac{\hat{b}^{N_{\text{in}}-1}}{2\pi} B\left[1 - \left(\frac{\Delta}{\hat{b}}\right)^2; \frac{N_{\text{in}}}{2}, \frac{1}{2}\right] \tag{19}$$

where $\Delta = \frac{1}{2}\|\mathbf{x}_i - \mathbf{x}_j\|_2$ and $\hat{b} = \sin(\arccos(b))$ (details in Appendix B.2).

In conclusion, an infinitely large SDM with sparse internal representations $\boldsymbol{\phi}_{\text{SDM}}$, can be represented as a suboptimal case of a feed-forward SVM network with a translation-invariant kernel.

3.3 The modern Hopfield network is a recurrent SVM network

The Hopfield network [23] is, arguably, the most well-known model of auto-associative memory. In its modern form [32], it is a recurrent network of N neurons with the state $\mathbf{s}^{(t)}$, whose dynamics are governed by the energy and state update rule

$$E = -\sum_{\mu}^{M} F\left(\sum_{i}^{N} \xi_i^\mu s_i^{(t)}\right), \quad s_i^{(t+1)} = \text{sgn}\left[\sum_{\mu}^{M} \xi_i^\mu F'\left(\sum_{j \neq i}^{N} \xi_j^\mu s_j^{(t)}\right)\right] \tag{20}$$

where F is a smooth function, typically a sigmoid, polynomial, or exponential. This "generalized" Hopfield model has a long history [see, e.g., 1, 19, 34] but has received renewed attention in recent years under the name *modern Hopfield network* (MHN) or *dense associative memory* [15, 32]. By comparing Eq. 20 with Eq. 12, the state update of the MHN can be identified as a special case of a suboptimal recurrent SVM network in the kernel representation, with $k = F'$, $\mathbf{A} = \mathbf{1}$, and $\boldsymbol{\theta} = \mathbf{0}$ (since $f = 0.5$). With a linear $F'(x) = x$, the MHN reduces to the classical Hopfield network, which is a special case of the linear SVM network in Eq. 13.

Capacity. The storage capacity of the MHN has been shown to depend on the shape of F'. In the linear case, the capacity is famously limited to $\sim 0.1N$ patterns, depending on the precision of retrieval [2, 39]. If, on the other hand, F' is polynomial with degree p, the capacity scales as $M_{\max} \sim \mathcal{O}(N^p)$ [32]. Analogously, an exponential F' endows the network with a capacity $M_{\max} \sim \mathcal{O}(e^N)$ [15]. From the perspective of the kernel attractor framework, this scaling directly follows from the analysis in Sec. 3.1 with $k = F'$.

Generalization. Viewing the MHN as a recurrent network of SVMs can also facilitate a more intuitive understanding of its ability to generalize, when used as a conventional classifier. In this setting, one designates a subset of the neurons as input units, and the remaining neurons as outputs.

Given a set of input-output associations, one optimizes the memory patterns $\boldsymbol{\xi}^\mu$ using, for example, gradient descent. Such an experiment was performed by Krotov and Hopfield [32] on the MNIST data set, using a polynomial non-linearity $F(x) = x^p$. Their results showed that the test error first improved as p increased from 2 to 3, but later deteriorated for high degrees, like $p = 20$. While it may be difficult to explain this behavior within an energy-based framework, it is entirely expected when viewed from the SVM perspective: a kernel of low polynomial degree has too few degrees of freedom to fit the classification boundary in the training set, causing *underfitting*, while a polynomial of too high degree grants the model too much flexibility, which results in *overfitting*.

Online learning. Recently, Tyulmankov et al. [59] proposed a biologically plausible online learning algorithm to train the weights in an MHN. Depending on the implementation, the resulting storage capacity scales as either $\sim 0.16N$ or $\sim N$. In a comment on the discrepancy between these results and the maximum capacity $\sim 2N$, the authors noted that they are not aware of a learning algorithm that is able to reach the upper bound. Here, the perspective of kernel attractor networks can be particularly helpful, as many of the algorithms that have been developed over the past two decades to optimize SVMs can be utilized for MHNs as well. For example, a network formulated in the feature representation can be trained with the stochastic batch perceptron rule [12, 31], the passive aggressive rules [14], the minnorm rule [4], as well as with likelihood maximization applied to logistic regression [26, 42, 54]. In the kernel representation, two of the most well-known online algorithms for training linear and non-linear SVMs are the Adatron [3] and the Kernel-Adatron [17]. A performance comparison between online learning and the modern Hopfield learning rule in an SVM network can be found in Appendix C.

The pseudoinverse learning rule. The coefficients in $\mathbf{A}$ are, in general, computed numerically, and cannot be written in closed form. However, in the special case when Eq. 8 is underdetermined, meaning $M < N_\phi$, a closed-form (but suboptimal) solution can be obtained using the *least-squares SVM* method [55]. The result is a generalized form of the *pseudoinverse learning rule* [45]. See Appendix D for details.

4 Kernel attractor networks for continuous patterns

4.1 *Auto*-associative memory as a recurrent interpolation network

So far, we have considered memory models designed to store only bipolar patterns. We now relax this constraint and allow patterns to be continuous-valued. We first observe that any set of patterns $\mathbf{X} \in \mathbb{R}^{N \times M}$ can be made fixed points of the dynamics by training each neuron i to interpolate ξ_i^μ when the rest of the network is initialized in $\boldsymbol{\xi}^\mu$, for every pattern μ. Assuming that the model is equipped with a kernel that allows for each fixed point to also be attracting, we can ensure that a lower bounding estimate of the size of the attractor basin is maximized by finding the interpolation with minimum weight norms (see Appendix E.1 for proof). These results are summarized below.

Property 4 (Robust auto-associative memory with continuous patterns)**.** *Suppose that the dynamics of a recurrent auto-associative memory network evolve according to the synchronous update rule*

$$\mathbf{s}^{(t+1)} = \mathbf{X}\mathbf{K}^\dagger K(\mathbf{X}, \mathbf{s}^{(t)}) \tag{21}$$

where $\mathbf{K} = K(\mathbf{X}, \mathbf{X}) = \boldsymbol{\phi}(\mathbf{X})^\top \boldsymbol{\phi}(\mathbf{X})$ *is the kernel matrix and* $\mathbf{K}^\dagger$ *the Moore-Penrose pseudoinverse, where* $\mathbf{K}^\dagger = \mathbf{K}^{-1}$ *if* $\boldsymbol{\phi}(\mathbf{X})$ *is full column rank. Then, the dynamics of the network is guaranteed to have the fixed points* $\mathbf{X}$*. Moreover, if the points are attracting, Eq. 21 maximizes a lower-bounding estimate of the size of the attractor basins.*

4.2 A recurrent SDM for continuous patterns

Memory models for continuous data have generally received less attention than their binary counterparts [24, 30]. Recently, however, Ramsauer et al. [52] proposed an energy-based model capable of storing an exponential number of continuous-valued patterns (we will refer to this model as the softmax network). While the structure of this model is similar to Eq. 21, it cannot be analyzed within the framework of Property 4, as it involves a kernel that is neither symmetric nor positive-definite [63].

Nonetheless, we will in this section demonstrate that it is possible to use conventional kernel methods to design an attractor network with similar properties as the softmax network. We generalize the SDM to continuous patterns and use a translation-invariant kernel with a fixed spatial scale r. For the sake of simplicity, we choose the exponential power kernel (Exp_β)

$$K_{\text{exp}_\beta}(\mathbf{x}_i, \mathbf{x}_j) = \exp\left[-\left(\frac{1}{r}\|\mathbf{x}_i - \mathbf{x}_j\|_2\right)^\beta\right] \tag{22}$$

where $\beta, r > 0$. These parameters determine the shape of the hyperspherical attractor basin that surrounds each pattern. While r roughly sets the radius of attraction, β represents an inverse temperature which changes the steepness of the boundary of the attractor basin. Moreover, as long as the patterns are unique, the kernel matrix is invertible and we have $\mathbf{K}^\dagger_{\text{exp}_\beta} = \mathbf{K}^{-1}_{\text{exp}_\beta}$ [41].

We will now analyze the noise robustness and storage capacity of this model. To make the analysis tractable, we will operate in the regime of low temperatures, meaning the limit $\beta \to \infty$. We first establish the following three properties.

Property 5.1 (The Exp_β network at zero temperature)**.** *Given a set of unique patterns $\{\boldsymbol{\xi}^\mu\}_{\mu=1}^M$ with $\min_{\mu,\nu\neq\mu}\|\boldsymbol{\xi}^\mu - \boldsymbol{\xi}^\nu\|_2 > r$, the state update rule for the Exp_β network at $\beta \to \infty$ reduces to*

$$\mathbf{s}^{(t+1)} = \mathbf{X}\,\Theta(r - \|\mathbf{X} - \mathbf{s}^{(t)}\|_2) \tag{23}$$

where $\Theta(\cdot)$ is the Heaviside function with $\Theta(0) = e^{-1}$ (see Appendix E.2.1).

Remark. In geometrical terms, Property 5.1 states that the boundary of the basin of attraction surrounding each pattern becomes a sharp $(N-1)$-dimensional hypersphere with radius r in the limit $\beta \to \infty$. For lower, finite β, the spherical boundary becomes increasingly fuzzy. From the perspective of an energy landscape, each pattern lies in an N-dimensional energy minimum with infinitely steep walls when $\beta \to \infty$. As β is lowered, the barriers become progressively smoother.

Property 5.2 (Convergence in one step)**.** *Given a set of unique patterns $\{\boldsymbol{\xi}^\mu\}_{\mu=1}^M$ with $\min_{\mu,\nu\neq\mu}\|\boldsymbol{\xi}^\mu - \boldsymbol{\xi}^\nu\|_2 > 2r$, the Exp_β network at $\beta \to \infty$, initialized at $\mathbf{s}^{(0)} = \boldsymbol{\xi}^\mu + \Delta\boldsymbol{\xi}$, will converge to $\boldsymbol{\xi}^\mu$ in one step if $\|\Delta\boldsymbol{\xi}\|_2 < r$.*

Property 5.3 (No spurious attractors)**.** *Given a set of unique patterns $\{\boldsymbol{\xi}^\mu\}_{\mu=1}^M$ with $\min_{\mu,\nu\neq\mu}\|\boldsymbol{\xi}^\mu - \boldsymbol{\xi}^\nu\|_2 > 2r$ and $\nexists\mu : \|\boldsymbol{\xi}^\mu\|_2 = r/(1-e^{-1})$, the only attractors of the dynamics of the Exp_β network at $\beta \to \infty$ are the points $\{\boldsymbol{\xi}^\mu\}_{\mu=1}^M$, together with $\mathbf{0}$ if $\nexists\mu : \|\boldsymbol{\xi}^\mu\|_2 \leq r$.*

Remark. Properties 5.2 and 5.3 can be shown to be true simply by inserting the expression $\mathbf{s}^{(0)} = \boldsymbol{\xi}^\mu + \Delta\boldsymbol{\xi}$ in Eq. 23. Assuming no overlaps between the basins of attraction, a quick calculation shows that $\mathbf{s}^{(1)} = \boldsymbol{\xi}^\mu$ if $\|\Delta\boldsymbol{\xi}\|_2 < r$. If, on the other hand, the network is initialized such that $\|\mathbf{s}^{(0)} - \boldsymbol{\xi}^\mu\|_2 > r, \forall\mu$, one always obtains $\mathbf{s}^{(2)} = \boldsymbol{\xi}^0$, where $\boldsymbol{\xi}^0$ is either $\mathbf{0}$ or the pattern closest to $\mathbf{0}$. In other words, the network recalls a pattern only if the initialization is close enough to it. If located far from *all* patterns, the network assumes an "agnostic" state, represented either by the origin or the pattern closest to the origin (if the origin happens to be located within a basin of attraction).

In the following two properties, we evaluate how the radius of attraction r determines the maximum input noise tolerance and storage capacity.

Property 6 (Robustness to white noise)**.** *Assume that we are given a set of unique patterns $\boldsymbol{\xi}^1, \ldots, \boldsymbol{\xi}^M \sim \mathcal{N}(\mathbf{0}, \mathbf{I}_N)$ with $\min_{\mu,\nu\neq\mu}\|\boldsymbol{\xi}^\mu - \boldsymbol{\xi}^\nu\|_2 > 2r$, and that the Exp_β network is initialized in a distorted pattern $\mathbf{s}^{(0)} = \boldsymbol{\xi}^\mu + \boldsymbol{\epsilon}$, where $\boldsymbol{\epsilon} \sim \mathcal{N}(\mathbf{0}, \sigma^2\mathbf{I}_N)$. Then, at $\beta \to \infty$, the maximum noise variance $\sigma^2_{\max}$ with which $\boldsymbol{\xi}^\mu$ can be recovered in at least 50% of trials is*

$$\sigma^2_{\max} = r^2/N\ . \tag{24}$$

Property 7 (Exponential storage capacity)**.** *At $\beta \to \infty$, and for $N \gg 1$, the average maximum number of patterns sampled from $\mathcal{N}(\mathbf{0}, \mathbf{I}_N)$ that the Exp_β network can store and recall without errors is lower-bounded by*

$$M_{\max} \geq \sqrt{2\sqrt{\pi N}(1 - 2\sigma^2_{\max})}\exp\left[\frac{N(1-2\sigma^2_{\max})^2}{8}\right] \tag{25}$$

where $\sigma^2_{\max}$ is the maximum white noise variance tolerated by the network.

Remark. Proofs can be found in Appendices E.2.2 and E.2.3. Note that Property 7 is valid in the range $\sigma^2_{\max} \lesssim 1/2$. While the bounds are fairly tight at the upper end of the range, they become loose when $\sigma^2_{\max} \to 0$. In this regime, $r \to 0$, which allows for infinite storage capacity, as the risk of interference between patterns becomes highly unlikely when their radius of attraction is very small.

Comparison to the softmax network. When the patterns in $\mathbf{X}$ are randomly placed on a hypersphere instead of being normally distributed, the state update rule in Eq. 23 reduces to the form $\mathbf{s}^{(t+1)} = \mathbf{X}\,\Theta(\mathbf{X}^\top \mathbf{s}^{(t)} - \theta)$, where θ is a fixed threshold. The capacity remains exponential (see Appendix E.3.1), but the basin of attraction surrounding each pattern now forms a spherical cap. We can compare this to the softmax network at zero temperature, $\mathbf{s}^{(t+1)} = \lim_{\beta\to\infty} \mathbf{X}\,\mathrm{softmax}(\beta \mathbf{X}^\top \mathbf{s}^{(t)}) = \mathbf{X}\arg\max(\mathbf{X}^\top \mathbf{s}^{(t)})$. The only difference between the two models is a replacement of Θ with $\arg\max$. This changes the shape of each attractor basin from a spherical cap to a Voronoi cell, so that the patterns parcellate the surface of the hypersphere into a Voronoi diagram. The extent of each basin is now no longer radially symmetric around the pattern, but instead maximal in all directions, without overlapping another basin (see Appendix E.5). The softmax network can be seen as an interpolation (Eq. 21) with $K = \mathrm{softmax}$ and the approximation $\mathbf{K} \approx \mathbf{I}_M$.

5 Discussion

Biological interpretation. Kernel attractor networks can be mapped to the anatomical properties of biological neurons. Consider an individual neuron in the feature representation of the recurrent network (Eq. 9). The state of neighboring neurons $\mathbf{s}$ is first transformed through $\boldsymbol{\phi}(\mathbf{s})$ and thereafter projected to the neuron through the weight matrix $(\mathbf{A} \odot \mathbf{X})\boldsymbol{\phi}(\mathbf{X})^\top$. When the kernel is polynomial of degree p, so that $K(\mathbf{x}_i, \mathbf{x}_j) = (\mathbf{x}_i^\top \mathbf{x}_j + 1)^p$, the transformation $\boldsymbol{\phi}(\mathbf{s})$ consists of all elements in $\mathbf{s}$ and their cross-terms, up to degree p. The input to each neuron, in other words, consists of the states of all other neurons, as well as all possible combinations of their multiplicative interactions. This neuron model can be viewed as a generalized form of, for example, the multiconnected neuron [44], the clusteron [40], or the sigma-pi unit [53, p. 73]. These are all perceptrons that include multiplicative input interactions as a means to model synaptic clustering on non-linear dendrites [50] (see Fig. 1).

In the kernel representation (Eq. 10), each neuron is, again, implicitly comprised of a two-stage process, whereby the raw input $\mathbf{s}$ is first transformed through the function $K(\mathbf{X}, \mathbf{s})$ and then projected through the weight matrix $\mathbf{A} \odot \mathbf{X}$. For any inner-product kernel $K = k(\mathbf{x}_i^\top \mathbf{x}_j)$, this representation can be directly identified as a two-layer neural network, where the hidden layer is defined by the weights $\mathbf{X}$ and the activation function k. This interpretation of the recurrent network was recently proposed in [32, 33] and discussed in relation to hippocampal-cortical interactions involved in memory storage and recall; it is particularly reminiscent of the hippocampal indexing theory [5, 56]. However, the kernel representation can also be viewed as a network in which each *individual* neuron is a generalized form of the two-layered pyramidal cell model [48, 49]. This was originally proposed as an abstract neuron model augmented with non-linear dendritic processing [38]. It should be noted, however, that the idea of interpreting kernel methods as neural networks has a longer history, and has been extensively analyzed in the case of, for example, radial basis functions [46, 47]. For further details, see Appendix F.

Summary. We have shown that conventional kernel methods can be used to derive the weights for hetero- and auto-associative memory networks storing binary or continuous-valued patterns with maximal noise tolerance. The result is a family of optimal memory models, which we call *kernel attractor networks*, which includes the SDM and MHN as special cases. This unifying framework facilitates an intuitive understanding of the storage capacity of memory models and offers new ways to biologically interpret these in terms of non-linear dendritic integration. This work formalizes the links between kernel methods, attractor networks, and models of dendritic processing.

Future work. A unifying theoretical framework for memory modeling can be useful for the development of both improved bio-plausible memory models and for machine learning applications. First, recognizing that there exists online algorithms for training optimally noise-robust classifiers and adapting these to biological constraints can aid in the development of normative synaptic three-factor learning rules [21]. Second, the theoretical link between neuron models, kernel functions, and storage capacity enables one to fit kernel attractor networks to neurophysiological data and to analyze the computational properties of biophysically informed memory models. Finally, our unifying framework reveals that most memory models differ only in the choice of kernel (model complexity) and Lagrange parameters (model precision). This categorization simplifies the tailoring of memory models to their application, and allows for the design of models whose properties fundamentally depart from kernel attractor networks, by choosing kernels not associated with a reproducing kernel Hilbert space.

References

[1] Abbott, L. F. and Arian, Y. (1987). "Storage capacity of generalized networks". *Physical Review A* 36, pp. 5091–5094.

[2] Amit, D. J., Gutfreund, H., and Sompolinsky, H. (1985). "Storing infinite numbers of patterns in a spin-glass model of neural networks". *Physical Review Letters* 55, pp. 1530–1533.

[3] Anlauf, J. K. and Biehl, M. (1989). "The AdaTron: an adaptive perceptron algorithm". *Europhysics Letters* 10, pp. 687–692.

[4] Bansal, Y., Advani, M., Cox, D. D., and Saxe, A. M. (2018). "Minnorm training: an algorithm for training over-parameterized deep neural networks". Preprint. arXiv: 1806.00730.

[5] Barry, D. N. and Maguire, E. A. (2019). "Remote memory and the hippocampus: a constructive critique". *Trends in Cognitive Sciences* 23, pp. 128–142.

[6] Boros, G. and Moll, V. (2004). *Irresistible integrals: symbolics, analysis and experiments in the evaluation of integrals*. Cambridge University Press.

[7] Bricken, T. and Pehlevan, C. (2021). "Attention approximates sparse distributed memory". *Advances in Neural Information Processing Systems 34*.

[8] Chen, L. and Xu, S. (2020). "Deep neural tangent kernel and Laplace kernel have the same RKHS". *Proceedings of the 2021 International Conference on Learning Representations*.

[9] Cho, Y. and Saul, L. (2009). "Kernel methods for deep learning". *Advances in Neural Information Processing Systems 22*.

[10] Chou, P. A. (1989). "The capacity of the Kanerva associative memory". *IEEE Transactions on Information Theory* 35, pp. 281–298.

[11] Cortes, C. and Vapnik, V. (1995). "Support-vector networks". *Machine Learning* 20, pp. 273–297.

[12] Cotter, A., Shalev-Shwartz, S., and Srebro, N. (2012). "The kernelized stochastic batch perceptron". *Proceedings of the 29th International Conference on Machine Learning*, pp. 739–746.

[13] Cover, T. M. (1965). "Geometrical and statistical properties of systems of linear inequalities with applications in pattern recognition". *IEEE Transactions on Electronic Computers* EC-14, pp. 326–334.

[14] Crammer, K., Dekel, O., Keshet, J., Shalev-Shwartz, S., and Singer, Y. (2006). "Online passive-aggressive algorithms". *Journal of Machine Learning Research* 7, pp. 551–585.

[15] Demircigil, M., Heusel, J., Löwe, M., Upgang, S., and Vermet, F. (2017). "On a model of associative memory with huge storage capacity". *Journal of Statistical Physics* 168, pp. 288–299.

[16] Forrest, B. M. (1988). "Content-addressability and learning in neural networks". *Journal of Physics A: Mathematical and General* 21, pp. 245–255.

[17] Frieß, T.-T., Cristianini, N., and Campbell, C. (1998). "The Kernel-Adatron algorithm: a fast and simple learning procedure for support vector machines". *Proceedings of the 15th International Conference on Machine Learning*, pp. 188–196.

[18] Gardner, E. (1987a). "Maximum storage capacity in neural networks". *Europhysics Letters* 4, pp. 481–485.

[19] Gardner, E. (1987b). "Multiconnected neural network models". *Journal of Physics A: Mathematical and General* 20, pp. 3453–3464.

[20] Gardner, E. (1988). "The space of interactions in neural network models". *Journal of Physics A: Mathematical and General* 21, pp. 257–270.

[21] Gerstner, W., Lehmann, M., Liakoni, V., Corneil, D., and Brea, J. (2018). "Eligibility traces and plasticity on behavioral time scales: experimental support of neohebbian three-factor learning rules". *Frontiers in Neural Circuits* 12.

[22] Graves, A., Wayne, G., and Danihelka, I. (2014). "Neural Turing machines". Preprint. arXiv:1410.5401.

[23] Hopfield, J. J. (1982). "Neural networks and physical systems with emergent collective computational abilities". *Proceedings of the National Academy of Sciences* 79, pp. 2554–2558.

[24] Hopfield, J. J. (1984). "Neurons with graded response have collective computational properties like those of two-state neurons". *Proceedings of the National Academy of Sciences* 81, pp. 3088–3092.

[25] Jacot, A., Gabriel, F., and Hongler, C. (2018). "Neural tangent kernel: convergence and generalization in neural networks". *Advances in Neural Information Processing Systems 31*.

[26] Ji, Z., Srebro, N., and Telgarsky, M. (2021). "Fast margin maximization via dual acceleration". *Proceedings of the 38th International Conference on Machine Learning*, pp. 4860–4869.

[27] Kanerva, P. (1988). *Sparse distributed memory*. MIT Press.

[28] Keeler, J. D. (1988). "Comparison between Kanerva's SDM and Hopfield-type neural networks". *Cognitive Science* 12, pp. 299–329.

[29] Kepler, T. B. and Abbott, L. F. (1988). "Domains of attraction in neural networks". *Journal de Physique* 49, pp. 1657–1662.

[30] Koiran, P. (1994). "Dynamics of discrete time, continuous state Hopfield networks". *Neural Computation* 6, pp. 459–468.

[31] Krauth, W. and Mezard, M. (1987). "Learning algorithms with optimal stability in neural networks". *Journal of Physics A: Mathematical and General* 20, pp. L745–L752.

[32] Krotov, D. and Hopfield, J. J. (2016). "Dense associative memory for pattern recognition". *Advances in Neural Information Processing Systems 29*, pp. 1172–1180.

[33] Krotov, D. and Hopfield, J. J. (2020). "Large associative memory problem in neurobiology and machine learning". *Proceedings of the 9th International Conference on Learning Representations*.

[34] Lee, Y. C., Doolen, G., Chen, H. H., Sun, G. Z., Maxwell, T., Lee, H. Y., and Giles, C. L. (1986). "Machine learning using a higher order correlation network". *Physica D: Nonlinear Phenomena* 22, pp. 276–306.

[35] Lee, Y. and Kim, W. C. (2014). *Concise formulas for the surface area of the intersection of two hyperspherical caps*. Technical Report. Department of Industrial and Systems Engineering, KAIST.

[36] Li, S. (2011). "Concise formulas for the area and volume of a hyperspherical cap". *Asian Journal of Mathematics and Statistics* 4, pp. 66–70.

[37] MacKay, D. J. C. (2003). *Information theory, inference and learning algorithms*. Cambridge University Press.

[38] Major, G., Larkum, M. E., and Schiller, J. (2013). "Active properties of neocortical pyramidal neuron dendrites". *Annual Review of Neuroscience* 36, pp. 1–24.

[39] McEliece, R., Posner, E., Rodemich, E., and Venkatesh, S. (1987). "The capacity of the Hopfield associative memory". *IEEE Transactions on Information Theory* 33, pp. 461–482.

[40] Mel, B. W. (1991). "The clusteron: toward a simple abstraction for a complex neuron". *Advances in Neural Information Processing Systems 4*, pp. 35–42.

[41] Micchelli, C. A. (1986). "Interpolation of scattered data: distance matrices and conditionally positive definite functions". *Constructive Approximation* 2, pp. 11–22.

[42] Nacson, M. S., Lee, J., Gunasekar, S., Savarese, P. H. P., Srebro, N., and Soudry, D. (2019). "Convergence of gradient descent on separable data". *Proceedings of the 22nd International Conference on Artificial Intelligence and Statistics*, pp. 3420–3428.

[43] Neal, R. M. (1996). "Priors for infinite networks". *Bayesian Learning for Neural Networks*. Ed. by Neal, R. M. Vol. 118. Lecture Notes in Statistics. Springer, pp. 29–53.

[44] Peretto, P. and Niez, J. J. (1986). "Long term memory storage capacity of multiconnected neural networks". *Biological Cybernetics* 54, pp. 53–63.

[45] Personnaz, L., Guyon, I., and Dreyfus, G. (1986). "Collective computational properties of neural networks: New learning mechanisms". *Physical Review A* 34, pp. 4217–4228.

[46] Poggio, T. and Girosi, F. (1990a). "Networks for approximation and learning". *Proceedings of the IEEE* 78, pp. 1481–1497.

[47] Poggio, T. and Girosi, F. (1990b). "Regularization algorithms for learning that are equivalent to multilayer networks". *Science* 247, pp. 978–982.

[48] Poirazi, P., Brannon, T., and Mel, B. W. (2003). "Pyramidal neuron as two-layer neural network". *Neuron* 37, pp. 989–999.

[49] Poirazi, P. and Mel, B. W. (2001). "Impact of active dendrites and structural plasticity on the memory capacity of neural tissue". *Neuron* 29, pp. 779–796.

[50] Polsky, A., Mel, B. W., and Schiller, J. (2004). "Computational subunits in thin dendrites of pyramidal cells". *Nature Neuroscience* 7, pp. 621–627.

[51] Radhakrishnan, A., Belkin, M., and Uhler, C. (2020). "Overparameterized neural networks implement associative memory". *Proceedings of the National Academy of Sciences* 117, pp. 27162–27170.

[52] Ramsauer, H., Schäfl, B., Lehner, J., Seidl, P., Widrich, M., Gruber, L., Holzleitner, M., Adler, T., Kreil, D., Kopp, M. K., Klambauer, G., Brandstetter, J., and Hochreiter, S. (2021). "Hopfield networks is all you need". *Proceedings of the 9th International Conference on Learning Representations*.

[53] Rumelhart, D. E. and McClelland, J. L. (1986). *Parallel distributed processing: explorations in the microstructure of cognition*. Vol. 1. MIT Press.

[54] Soudry, D., Hoffer, E., Nacson, M. S., Gunasekar, S., and Srebro, N. (2018). "The implicit bias of gradient descent on separable data". *The Journal of Machine Learning Research* 19, pp. 2822–2878.

[55] Suykens, J. and Vandewalle, J. (1999). "Least squares support vector machine classifiers". *Neural Processing Letters* 9, pp. 293–300.

[56] Teyler, T. J. and Rudy, J. W. (2007). "The hippocampal indexing theory and episodic memory: updating the index". *Hippocampus* 17, pp. 1158–1169.

[57] Tony Cai, T. and Jiang, T. (2012). "Phase transition in limiting distributions of coherence of high-dimensional random matrices". *Journal of Multivariate Analysis* 107, pp. 24–39.

[58] Tsai, Y.-H. H., Bai, S., Yamada, M., Morency, L.-P., and Salakhutdinov, R. (2019). "Transformer dissection: an unified understanding for transformer's attention via the lens of kernel". *Proceedings of the 2019 Conference on Empirical Methods in Natural Language Processing and the 9th International Joint Conference on Natural Language Processing (EMNLP-IJCNLP)*, pp. 4344–4353.

[59] Tyulmankov, D., Fang, C., Vadaparty, A., and Yang, G. R. (2021). "Biological learning in key-value memory networks". *Advances in Neural Information Processing Systems 34*.

[60] Vaswani, A., Shazeer, N., Parmar, N., Uszkoreit, J., Jones, L., Gomez, A. N., Kaiser, Ł., and Polosukhin, I. (2017). "Attention is all you need". *Advances in Neural Information Processing Systems 30*.

[61] Weston, J., Chopra, S., and Bordes, A. (2015). "Memory networks". *Proceedings of the 2015 International Conference on Learning Representations*.

[62] Williams, C. (1996). "Computing with infinite networks". *Advances in Neural Information Processing Systems 9*.

[63] Wright, M. A. and Gonzalez, J. E. (2021). "Transformers are deep infinite-dimensional non-Mercer binary kernel machines". Preprint. arXiv: 2106.01506.

[64] Wu, Y., Wayne, G., Graves, A., and Lillicrap, T. (2018). "The Kanerva machine: a generative distributed memory". *Proceedings of the 2018 International Conference on Learning Representations*.

Checklist

1. For all authors...
   (a) Do the main claims made in the abstract and introduction accurately reflect the paper's contributions and scope? [Yes]
   (b) Did you describe the limitations of your work? [Yes] *Our work is entirely theoretical and the limitations of our approach is treated in the main text when discussing, for example, the validity and assumptions of our derivations.*
   (c) Did you discuss any potential negative societal impacts of your work? [N/A]
   (d) Have you read the ethics review guidelines and ensured that your paper conforms to them? [N/A]
2. If you are including theoretical results...
   (a) Did you state the full set of assumptions of all theoretical results? [Yes] *This is included in all theoretical results, or in the explanatory text preceding them.*
   (b) Did you include complete proofs of all theoretical results? [Yes] *These can be found in the Appendix. Pointers to the correct sections are given in the main text.*
3. If you ran experiments...
   (a) Did you include the code, data, and instructions needed to reproduce the main experimental results (either in the supplemental material or as a URL)? [N/A]
   (b) Did you specify all the training details (e.g., data splits, hyperparameters, how they were chosen)? [N/A]
   (c) Did you report error bars (e.g., with respect to the random seed after running experiments multiple times)? [N/A]
   (d) Did you include the total amount of compute and the type of resources used (e.g., type of GPUs, internal cluster, or cloud provider)? [N/A]
4. If you are using existing assets (e.g., code, data, models) or curating/releasing new assets...
   (a) If your work uses existing assets, did you cite the creators? [N/A]
   (b) Did you mention the license of the assets? [N/A]
   (c) Did you include any new assets either in the supplemental material or as a URL? [N/A]
   (d) Did you discuss whether and how consent was obtained from people whose data you're using/curating? [N/A]
   (e) Did you discuss whether the data you are using/curating contains personally identifiable information or offensive content? [N/A]
5. If you used crowdsourcing or conducted research with human subjects...
   (a) Did you include the full text of instructions given to participants and screenshots, if applicable? [N/A]
   (b) Did you describe any potential participant risks, with links to Institutional Review Board (IRB) approvals, if applicable? [N/A]
   (c) Did you include the estimated hourly wage paid to participants and the total amount spent on participant compensation? [N/A]

Appendices

A Derivation of storage capacity scaling

Suppose that the kernel is a homogeneous polynomial of degree $p \ll N$, meaning $K(\mathbf{x}_i, \mathbf{x}_j) = (\mathbf{x}_i^\top \mathbf{x}_j)^p$. This implies that the associated feature map $\boldsymbol{\phi}(\mathbf{x})$ contains all monomials of degree p composed of the entries in $\mathbf{x}$. Moreover, given that each entry x_i is ± 1, each monomial in $\boldsymbol{\phi}$ can be written as an interaction term of the form $x_1^{p_1} x_2^{p_2} \cdots x_N^{p_N}$, where $p_i \in \{0, 1\}$ and $\sum_i^N p_i \leq p$ (i.e., no factor x_i has an exponent higher than 1 and the sum of exponents is $\leq p$). The reason for this is that

$$x_i^{n_i} = \begin{cases} 1\,, & \text{if } n_i \text{ even} \\ x_i\,, & \text{if } n_i \text{ odd}\,. \end{cases} \tag{26}$$

The number of unique interaction terms of precisely degree p (the highest degree) is $\binom{N}{p}$. As the binomial coefficient is known to be bounded according to

$$\left(\frac{N}{p}\right)^p \leq \binom{N}{p} \leq \left(\frac{Ne}{p}\right)^p \tag{27}$$

we obtain $\binom{N}{p} \sim \mathcal{O}(N^p)$, for p fixed. Thus, the effective dimensionality of $\boldsymbol{\phi}$ scales like $\mathcal{O}(N^p)$.

For the exponential kernel $K(\mathbf{x}_i, \mathbf{x}_j) = \exp(\mathbf{x}_i^\top \mathbf{x}_j) = \sum_{p=0}^{\infty} (\mathbf{x}_i^\top \mathbf{x}_j)^p / p!$, we first note that the monomials in $\boldsymbol{\phi}$ now will be interaction terms of all degrees $p = 0, \ldots, N$. No monomial of degree $p > N$ will be possible. The total number of unique interaction terms will therefore be

$$\sum_{p=0}^{N} \binom{N}{p} = 2^N = e^{N \log 2} \tag{28}$$

where the first equality can be found in [6, p. 14]. This gives us an effective dimensionality of $\boldsymbol{\phi}$ that scales like $\mathcal{O}(e^N)$.

B Kernel of an infinite SDM on the hypersphere

B.1 Derivation of Eq. 18.

We follow the same steps as [7], with additional simplifications towards the end. As stated in the main text, we seek to calculate the overlapping area of two hyperspherical caps. A formula for this can be found in [35], and can be written as

$$A_\cap = A_\triangledown(R, \alpha_{\min}, \alpha_2) + A_\triangledown(R, \alpha_v - \alpha_{\min}, \alpha_1) \tag{29}$$

where

$$A_\triangledown(R, \alpha_{\min}, \alpha_2) = \frac{\pi^{\frac{N_{\text{in}}-1}{2}}}{\Gamma(\frac{N_{\text{in}}-1}{2})} R^{N_{\text{in}}-1} \int_{\alpha_{\min}}^{\alpha_2} \sin(\varphi)^{N_{\text{in}}-2} I_{1-\frac{\tan^2(\alpha_{\min})}{\tan^2(\varphi)}} \left[\frac{N_{\text{in}}-2}{2}, \frac{1}{2}\right] \mathrm{d}\varphi \tag{30}$$

where R is the radius, I is the regularized incomplete Beta function, and

$$\alpha_1 = \alpha_2 = \arccos(b) \tag{31}$$

$$\alpha_v = \arccos(\mathbf{x}_i^\top \mathbf{x}_j) \tag{32}$$

$$\alpha_{\min} = \arctan\left(\frac{\cos(\alpha_1)}{\cos(\alpha_2)\sin(\alpha_v)} - \frac{1}{\tan(\alpha_v)}\right) \tag{33}$$

$$R = 1\,. \tag{34}$$

We insert Eq. 31 in 33 and obtain

$$\alpha_{\min} = \arctan\left(\frac{1}{\sin(\alpha_v)} - \frac{\cos(\alpha_v)}{\sin(\alpha_v)}\right) = \arctan\left(\tan\left(\frac{\alpha_v}{2}\right)\right) = \frac{\alpha_v}{2} \tag{35}$$

where we have used $\tan(\alpha/2) = (1-\cos(\alpha))/\sin(\alpha)$. Eq. 35 also follows from the symmetry of the problem. This result yields

$$A_\cap = A_\triangledown(R, \alpha_{\min}, \alpha_2) + A_\triangledown(R, \alpha_v - \alpha_{\min}, \alpha_1) = 2A_\triangledown(R, \alpha_{\min}, \alpha_1) \ . \tag{36}$$

We rewrite the regularized incomplete Beta function as

$$I_{1-\frac{\tan^2(\alpha_{\min})}{\tan^2(\varphi)}}\left[\frac{N_{\text{in}}-2}{2}, \frac{1}{2}\right] = \frac{\Gamma(\frac{N_{\text{in}}-1}{2})}{\Gamma(\frac{N_{\text{in}}-2}{2})\Gamma(\frac{1}{2})} B\left[1 - \frac{\tan^2(\alpha_{\min})}{\tan^2(\varphi)}; \frac{N_{\text{in}}-2}{2}, \frac{1}{2}\right] \tag{37}$$

where B is the incomplete Beta function. The area of an $(N_{\text{in}}-1)$-dimensional hypersphere is

$$A_\circ = \frac{2\pi^{\frac{N_{\text{in}}}{2}}}{\Gamma(\frac{N_{\text{in}}}{2})} R^{N_{\text{in}}-1} \ . \tag{38}$$

We insert Eq. 37 in 30 and use the result in Eq. 36. Using the notation $\alpha_b = \alpha_1$ and $\alpha_x = \alpha_{\min}$, and the identities

$$\frac{\Gamma(\frac{N_{\text{in}}}{2})}{\Gamma(\frac{N_{\text{in}}-2}{2})} = \frac{N_{\text{in}}-2}{2}, \quad \Gamma\left(\frac{1}{2}\right) = \sqrt{\pi} \ , \tag{39}$$

the ratio between the overlapping area of the hyperspherical caps and the complete are of the hypersphere can now be calculated as

$$\frac{A_\cap}{A_\circ} = \frac{N_{\text{in}}-2}{2\pi} \int_{\alpha_x}^{\alpha_b} \sin(\varphi)^{N_{\text{in}}-2} B\left[1 - \frac{\tan^2(\alpha_x)}{\tan^2(\varphi)}; \frac{N_{\text{in}}-2}{2}, \frac{1}{2}\right] \mathrm{d}\varphi \ . \tag{40}$$

B.2 Derivation of Eq. 19.

For a large bias $b \gtrsim 0.9$, which is equivalent to a small angle $\alpha_b = \arccos(b)$, the hyperspherical caps surrounding $\mathbf{x}_i$ and $\mathbf{x}_j$ will be very small in relation to the whole hypersphere. In this case, we can neglect the curvature of the hyperspherical surface and project the area of the hyperspherical cap to the plane that cuts through the rims of the cap. This projection is a $(N_{\text{in}}-1)$-dimensional hyperball (we will refer to it as a mini-ball). In three dimensions, for example, the projection of a spherical cap to the plane constitutes a disk, which is a 2-dimensional ball. The radius of each mini-ball is

$$\hat{b} = \sin(\arccos(b)) \tag{41}$$

and the half-distance between the centers of the mini-balls is

$$\Delta = \frac{1}{2}\|\mathbf{x}_i - \mathbf{x}_j\|_2 \ . \tag{42}$$

We estimate the overlapping area of the hyperspherical caps by calculating the overlapping volume of the mini-balls in $(N_{\text{in}}-1)$ dimensions. A formula for the overlapping volume of two hyperballs can be found in [36] and is

$$V_\cap = \frac{\pi^{\frac{N_{\text{in}}-1}{2}}}{\Gamma(\frac{N_{\text{in}}+1}{2})} \hat{b}^{N_{\text{in}}-1} I_{1-\left(\frac{\Delta}{\hat{b}}\right)^2}\left[\frac{N_{\text{in}}}{2}, \frac{1}{2}\right] \ . \tag{43}$$

We rewrite the regularized incomplete Beta function as

$$I_{1-\left(\frac{\Delta}{2\hat{b}}\right)^2}\left[\frac{N_{\text{in}}}{2}, \frac{1}{2}\right] = \frac{\Gamma(\frac{N_{\text{in}}+1}{2})}{\Gamma(\frac{N_{\text{in}}}{2})\Gamma(\frac{1}{2})} B\left[1 - \left(\frac{\Delta}{\hat{b}}\right)^2; \frac{N_{\text{in}}}{2}, \frac{1}{2}\right] \tag{44}$$

and insert Eq. 44 in 43. The ratio between the overlapping area of the hyperspherical caps and the complete area of the hypersphere can now be estimated as

$$\frac{A_\cap}{A_\circ} \approx \frac{V_\cap}{A_\circ} = \frac{\hat{b}^{N_{\text{in}}-1}}{2\pi} B\left[1 - \left(\frac{\Delta}{\hat{b}}\right)^2; \frac{N_{\text{in}}}{2}, \frac{1}{2}\right] \ . \tag{45}$$

A comparison of the exact solution in Eq. 40 and the approximation in Eq. 45 can be seen in Fig. B.1.

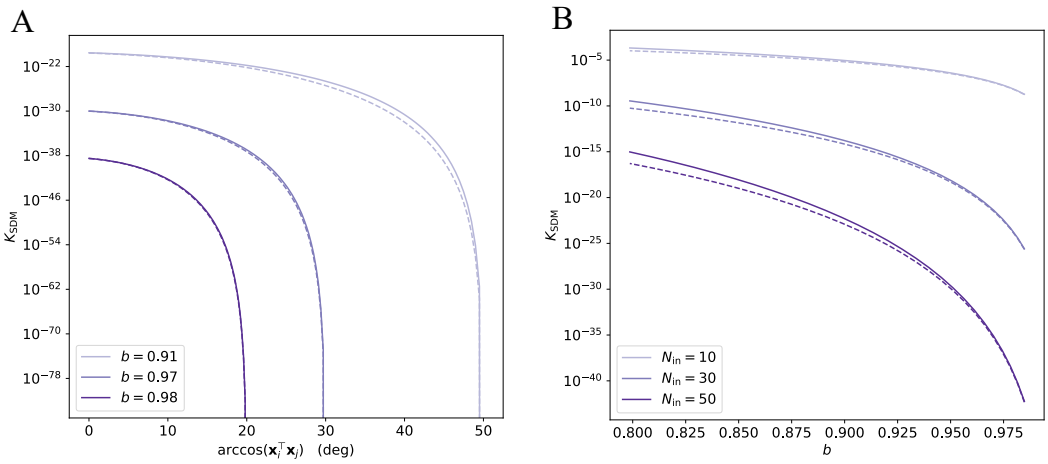

Figure B.1: Plot of the kernel of an infinite SDM on the hypersphere, $K_{\mathrm{SDM}}(\mathbf{x}_i, \mathbf{x}_j)$, as a function of (A) the angle between $\mathbf{x}_i$ and $\mathbf{x}_j$, and (B) the bias b. Solid lines represent the exact solution in Eq. 40, and dashed lines the approximation in Eq. 45. Parameter values: (A) $N_{\mathrm{in}} = 50$; (B) $\arccos(\mathbf{x}_i^\top \mathbf{x}_j) = \arccos(b)$.

C Online learning in an SVM network

We will in this section compare the noise tolerance of a single neuron in an SVM network when trained with an online learning rule, and when configured according to the MHN. First, we choose to equip the neuron with the feature map $\boldsymbol{\phi}_{\mathrm{pairs}}(\mathbf{x})$, which consists of all unique pairs of cross-terms $x_i x_j$, $i \neq j$. This yields a storage capacity scaling of $\mathcal{O}(N^2)$, and we therefore parameterize the storage load as M/N^2. We train the weights of the neuron either with the *stochastic batch perceptron* [12] or with the one-shot learning rule of the MHN, which is obtained by setting $\alpha^\mu = 1, \forall \mu$, in Eq. 4, that is

$$\mathbf{w} = \sum_{\mu}^{M} \xi_{\mathrm{out}}^\mu \boldsymbol{\phi}(\boldsymbol{\xi}_{\mathrm{in}}^\mu) \ . \tag{46}$$

Finally, we quantify the noise tolerance as the minimum Euclidean distance between the neuron's decision boundary and the patterns $\{\boldsymbol{\xi}_{\mathrm{in}}^\mu\}_{\mu=1}^M$. This is equivalent to the minimum classification margin, defined as

$$\gamma = \min_{\mu} \frac{\xi_{\mathrm{out}}^\mu (\mathbf{w}^\top \boldsymbol{\xi}_{\mathrm{in}}^\mu)}{\|\mathbf{w}\|_2} \ . \tag{47}$$

We are only interested in the performance regime where all patterns are correctly recalled (i.e., correctly classified). This means that we only compare positive margins, since a negative margin indicates that there is one or more patterns that no longer can be correctly recalled. The results are plotted in Fig. C.1, and demonstrate that the margin for the MHN quickly drops with increasing load, while the online learning rule achieves a margin close to the theoretical optimum derived by Gardner [20]. Moreover, as the maximum storage capacity $M_{\max}$ of each learning rule can be found at the intersection between the margin curve and $\gamma = 0$, the capacity of the online rule can be seen to be much higher than that of the MHN, and reaches close to $2D_{\mathrm{VC}}$.

D Generalized pseudoinverse rule

When the network is linear and underdetermined, meaning $M < N$, we can make sure that all patterns are attractors by modeling each neuron as a *least-squares SVM* [55] instead of a conventional SVM, so that the weights satisfy

$$\min_{\mathbf{w}} \|\mathbf{w}_i\|_2 \quad \text{s.t.} \quad \mathbf{w}_i^\top \boldsymbol{\xi}^\mu = \xi_i^\mu, \quad \forall \mu, i \ . \tag{48}$$

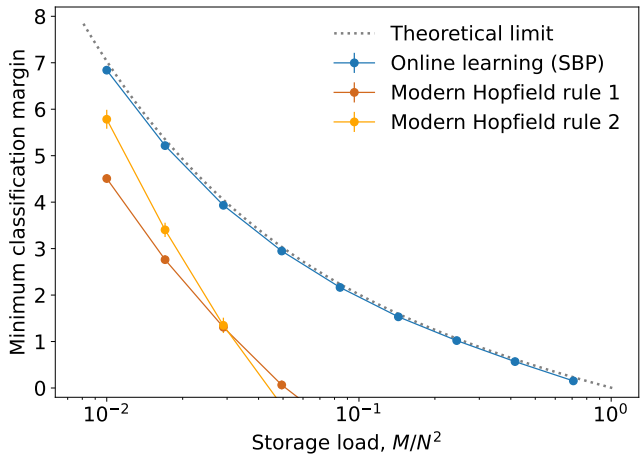

Figure C.1: Plot of the minimum classification margin (mean $\pm$ s.e.m. over 20 simulations) as a function of the storage load for a single SVM neuron with $N = 10^2$ inputs, trained with the stochastic batch perceptron (SBP) and the modern Hopfield rule. While the SBP and rule 1 use feature map $\boldsymbol{\phi}_{\text{pairs}}$, we also include rule 2 which uses the kernel $K(\mathbf{x}_i, \mathbf{x}_j) = (\mathbf{x}_i^\top \mathbf{x}_j)^2$, whose feature map differs slightly from $\boldsymbol{\phi}_{\text{pairs}}$. SBP hyperparameters: learning rate $= 10^{-5}$, weight updates $= 20M$.

This is a minimum-norm interpolation problem, and yields the solution

$$\mathbf{s}^{(t+1)} = \text{sgn}\left[\mathbf{X}\mathbf{K}^\dagger \mathbf{X}^\top \mathbf{s}^{(t)}\right] = \text{sgn}\left[\mathbf{X}\mathbf{X}^\dagger \mathbf{s}^{(t)}\right] \tag{49}$$

where $\mathbf{K} = \mathbf{X}^\top \mathbf{X}$ is the *kernel matrix* and $\mathbf{K}^\dagger$ its Moore-Penrose pseudoinverse, and where we have used the property $\mathbf{K}^\dagger \mathbf{X}^\top = (\mathbf{X}^\top \mathbf{X})^\dagger \mathbf{X}^\top = \mathbf{X}^\dagger$. This is the *pseudoinverse learning rule* [45].

The derivation can be extended to MHNs by performing interpolation on the feature map $\boldsymbol{\phi}(\boldsymbol{\xi}^\mu)$. Assuming that the problem is still underdetermined, so that $M < N_\phi$, we aim to find the weights

$$\min_{\mathbf{w}} \|\mathbf{w}_i\|_2 \quad \text{s. t.} \quad \mathbf{w}_i^\top \boldsymbol{\phi}(\boldsymbol{\xi}^\mu) = \xi_i^\mu, \quad \forall \mu, i \tag{50}$$

which, analogously to the linear case, produces the optimal state update

$$\mathbf{s}^{(t+1)} = \text{sgn}\left[\mathbf{X}\mathbf{K}^\dagger K(\mathbf{X}, \mathbf{s}^{(t)})\right] \tag{51}$$

where $\mathbf{K} = K(\mathbf{X}, \mathbf{X}) = \boldsymbol{\phi}(\mathbf{X})^\top \boldsymbol{\phi}(\mathbf{X})$. This can, again, be simplified to

$$\mathbf{s}^{(t+1)} = \text{sgn}\left[\mathbf{X}\boldsymbol{\phi}(\mathbf{X})^\dagger \boldsymbol{\phi}(\mathbf{s}^{(t)})\right] \tag{52}$$

where we can identify the weight matrix $\mathbf{W} = \mathbf{X}\boldsymbol{\phi}(\mathbf{X})^\dagger$. This is the *generalized pseudoinverse learning rule*. Note that, if the feature-expanded patterns $\{\boldsymbol{\phi}(\boldsymbol{\xi}^\mu)\}_{\mu=1}^M$ are linearly independent, the kernel matrix is invertible and we have $\mathbf{K}^\dagger = \mathbf{K}^{-1}$.

E The kernel attractor network for continuous patterns

E.1 Minimum norm interpolation and attractor basin size

Proof of Property 4. In this setting, each neuron is modeled as linear regressor whose state is updated according to

$$s_i^{(t+1)} = \mathbf{w}_i^\top \boldsymbol{\phi}(\mathbf{s}^{(t)}) \ . \tag{53}$$

All patterns $\mathbf{X}$ are guaranteed to be fixed points of the dynamics by finding the weights that satisfy

$$\xi_i^\mu = \mathbf{w}_i^\top \boldsymbol{\phi}(\boldsymbol{\xi}^\mu), \quad \forall \mu, i \ . \tag{54}$$

In order for each pattern to also be an attractor, the weights must satisfy the added constraint

$$\|\mathbf{J}_s(\mathbf{s}_1)\|_2 \Big|_{\mathbf{s}_0 = \boldsymbol{\xi}^\mu} < 1, \quad \forall \mu \tag{55}$$

where we have used the shorthand $\mathbf{s}_1 = \mathbf{s}^{(1)}$, $\mathbf{s}_0 = \mathbf{s}^{(0)}$, and $\mathbf{J}_s$ is the Jacobian with respect to $\mathbf{s}_0$. Eq. 55 states that the spectral norm of the Jacobian of the state update rule must be less than 1 when evaluated in each pattern. This ensures that the fixed points $\{\boldsymbol{\xi}^\mu\}_{\mu=1}^M$ are stable attractors and, equivalently, that the state update rule is a contractive map in a region surrounding each pattern [51]. It is assumed that there exists a solution that satisfies both Eq. 54 and 55. The basin of attraction of a fixed point μ can be defined as the set of points $\mathcal{S}^\mu_{\text{edge}}$ in the open neighborhood of $\boldsymbol{\xi}^\mu$ satisfying

$$\mathcal{S}^\mu_{\text{edge}} = \{\mathbf{s}_0 : \|\mathbf{J}_s(\mathbf{s}_1)\|_2 < 1\} \; . \tag{56}$$

Given that the spectral norm of the Jacobian is upper bounded by

$$\|\mathbf{J}_s(\mathbf{s}_1)\|_2 \leq \|\mathbf{J}_s(\mathbf{s}_1)\|_F \tag{57}$$

where $\|\cdot\|_F$ is the Frobenius norm, we can obtain a lower bound of the extent of the basin of attraction with the set

$$\widehat{\mathcal{S}}^\mu_{\text{edge}} = \{\mathbf{s}_0 : \|\mathbf{J}_s(\mathbf{s}_1)\|_F < 1\} \; . \tag{58}$$

Since the Jacobian is given by

$$\mathbf{J}_s(\mathbf{s}_1) = \mathbf{W} \cdot \mathbf{J}_s(\boldsymbol{\phi}(\mathbf{s}_0)) \tag{59}$$

where $\mathbf{W} = (\mathbf{w}_1, \ldots, \mathbf{w}_N)^\top$, we obtain

$$\|\mathbf{J}_s(\mathbf{s}_1)\|_F = \|\mathbf{W} \cdot \mathbf{J}_s(\boldsymbol{\phi}(\mathbf{s}_0))\|_F \leq \|\mathbf{W}\|_F \cdot \|\mathbf{J}_s(\boldsymbol{\phi}(\mathbf{s}_0))\|_F \tag{60}$$

where the last expression is given by the Cauchy-Schwartz inequality. Since $\|\mathbf{J}_s(\boldsymbol{\phi}(\mathbf{s}_0))\|_F$ depends only on the kernel and the patterns, which are both fixed, Eq. 60 can only be minimized by finding a set of weights that minimize $\|\mathbf{W}\|_F$. This is achieved by the minimum norm interpolation, given by

$$\min_{\mathbf{w}_i} \|\mathbf{w}_i\|_2 \quad \text{s. t.} \quad \xi_i^\mu = \mathbf{w}_i^\top \boldsymbol{\phi}(\boldsymbol{\xi}^\mu), \quad \forall \mu, i \; . \tag{61}$$

The solution is stated in Eq. 21. This solution maximizes a lower bound of the attractor basin sizes by maximizing the size of the set $\widehat{\mathcal{S}}^\mu_{\text{edge}}$. □

E.2 Normally distributed patterns

E.2.1 Kernel at zero temperature

Proof of Property 5.1. Using the notation $\Delta = \|\boldsymbol{\xi}^\mu - \boldsymbol{\xi}^\nu\|_2$, we have that

$$\lim_{\beta\to\infty} \left(\frac{\Delta}{r}\right)^\beta = \begin{cases} 0 \; , & \Delta < r \\ 1 \; , & \Delta = r \\ \infty \; , & \Delta > r \end{cases} \tag{62}$$

from which it follows that

$$\lim_{\beta\to\infty} \exp\left[-\left(\frac{\Delta}{r}\right)^\beta\right] = \begin{cases} 1 \; , & \Delta < r \\ e^{-1} \; , & \Delta = r \\ 0 \; , & \Delta > r \end{cases} \tag{63}$$

which is equivalent to $\Theta(r - \Delta)$ with $\Theta(0) = e^{-1}$. We combine this with the assumption that the patterns are unique and that $\min_{\mu,\nu\neq\mu} \|\boldsymbol{\xi}^\mu - \boldsymbol{\xi}^\nu\|_2 > r$ and obtain

$$\lim_{\beta\to\infty} K_{\exp_\beta}(\boldsymbol{\xi}^\mu, \boldsymbol{\xi}^\nu) = \Theta(r - \|\boldsymbol{\xi}^\mu - \boldsymbol{\xi}^\nu\|_2) = \begin{cases} 1 \; , & \mu = \nu \\ 0 \; , & \mu \neq \nu \end{cases} \tag{64}$$

which can be written compactly as

$$\lim_{\beta\to\infty} \mathbf{K}_{\exp_\beta} = \mathbf{I}_M \; . \tag{65}$$

It directly follows that

$$\lim_{\beta\to\infty} \mathbf{K}^{-1}_{\exp_\beta} = \mathbf{I}_M^{-1} = \mathbf{I}_M \tag{66}$$

and, therefore,

$$\lim_{\beta\to\infty} \mathbf{X}\mathbf{K}^{-1}_{\exp_\beta} K_{\exp_\beta}(\mathbf{X}, \mathbf{s}^{(t)}) = \mathbf{X}\,\Theta(r^2 - \|\mathbf{X} - \mathbf{s}^{(t)}\|_2^2) \; . \tag{67}$$

□

E.2.2 Noise robustness

Proof of Property 6. With $\mathbf{s}^{(0)} = \boldsymbol{\xi}^\mu + \boldsymbol{\epsilon}$, we have

$$\|\boldsymbol{\xi}^\mu - \mathbf{s}^{(0)}\|_2^2 = \|\boldsymbol{\epsilon}\|_2^2 = \|\sigma\boldsymbol{\epsilon}_0\|_2^2 = \sigma^2\|\boldsymbol{\epsilon}_0\|_2^2 \tag{68}$$

where $\boldsymbol{\epsilon}_0 \sim \mathcal{N}(\mathbf{0}, \mathbf{I}_N)$, from which it follows that $\|\boldsymbol{\epsilon}_0\|_2^2$ is a random variable with a $\chi^2(N)$ distribution. According to the central limit theorem, we also have

$$\lim_{N\to\infty} \frac{\|\boldsymbol{\epsilon}_0\|_2^2 - N}{\sqrt{2N}} \sim \mathcal{N}(0,1) \tag{69}$$

where we have used the fact that each term in $\|\boldsymbol{\epsilon}_0\|_2^2$ is $\chi^2(1)$-distributed, and has mean 1 and variance 2. We will therefore make the approximation $\|\boldsymbol{\epsilon}_0\|_2^2 \sim \mathcal{N}(N, 2N)$ for large N. This gives us

$$\sigma^2\|\boldsymbol{\epsilon}_0\|_2^2 \sim \mathcal{N}(\sigma^2 N, 2\sigma^4 N)\ . \tag{70}$$

The original pattern $\boldsymbol{\xi}^\mu$ will only be recovered if $r^2 - \|\boldsymbol{\xi}^\mu - \mathbf{s}^{(0)}\|_2^2 \geq 0$, which is satisfied in at least 50% of trials if $r^2 \geq \sigma^2 N$. The maximum variance with which this type of recovery still holds is thus

$$\sigma^2_{\max} = r^2/N\ . \tag{71}$$

□

E.2.3 Storage capacity

Proof of Property 7. In the limit $\beta \to \infty$, the boundary of the basin of attraction surrounding each pattern is sharp. In this setting, we are guaranteed that each pattern can be recalled without errors as long as $\min_{i,j\neq i}\|\boldsymbol{\xi}^i - \boldsymbol{\xi}^j\|_2 > 2r$. We will therefore estimate the storage capacity by calculating the number of patterns, on average, that can be loaded into the network before at least two attractor basins overlap and the condition above is violated (see Fig. E.1).

We begin by observing that for two random patterns $\boldsymbol{\xi}^i, \boldsymbol{\xi}^j \sim \mathcal{N}(\mathbf{0}, \mathbf{I}_N)$, we have

$$\frac{1}{2}\|\boldsymbol{\xi}^i - \boldsymbol{\xi}^j\|_2^2 \sim \chi^2(N) \tag{72}$$

which, using the central limit theorem as in Eq. 69, can be approximated as $\mathcal{N}(N, 2N)$ for large N, thereby yielding

$$\|\boldsymbol{\xi}^i - \boldsymbol{\xi}^j\|_2^2 \sim \mathcal{N}(2N, 8N)\ . \tag{73}$$

We now assume that the squared Euclidean distance between each pair of patterns $\boldsymbol{\xi}^i, \boldsymbol{\xi}^j$ in a set of M given patterns $\{\boldsymbol{\xi}^\mu\}_{\mu=1}^M$ is an independent sample of a random variable, denoted Δ^2, which is distributed as in Eq. 73. This is, of course, an approximation which neglects that the pairwise distances between any set of points are inter-dependent. Nonetheless, for relatively large N and M, the approximation accurately describes the empirical distance distribution.

Relying on this assumption, the process of drawing M random patterns becomes equivalent to drawing $M(M-1)/2$ unique pairwise distances Δ^2 from the distance distribution. The probability of drawing a sample $\Delta^2 \leq 4r^2$ can be calculated using the cumulative distribution function for the standard normal distribution, given by $\Phi(x) = \frac{1}{2}\operatorname{erfc}(-x)$, according to

$$\mathbb{P}(\Delta^2 \leq 4r^2) = \frac{1}{2}\operatorname{erfc}\left(\frac{N - 2r^2}{2\sqrt{N}}\right)\ . \tag{74}$$

The average number of samples of Δ^2 one needs to draw before a sample satisfies $\Delta^2 \leq 4r^2$ is given by $\mathbb{P}(\Delta^2 \leq 4r^2)^{-1}$. This determines the maximum number of patterns that the network, on average, can store, according to

$$\frac{M_{\max}(M_{\max}-1)}{2} = \frac{1}{\mathbb{P}(\Delta^2 \leq 4r^2)}\ . \tag{75}$$

We combine this expression with the approximation $M_{\max}(M_{\max}-1) \approx M_{\max}^2$ (which holds for large $M_{\max}$) and Eq. 74, and obtain

$$M_{\max} = 2\operatorname{erfc}\left(\frac{N - 2r^2}{2\sqrt{N}}\right)^{-1/2}\ . \tag{76}$$

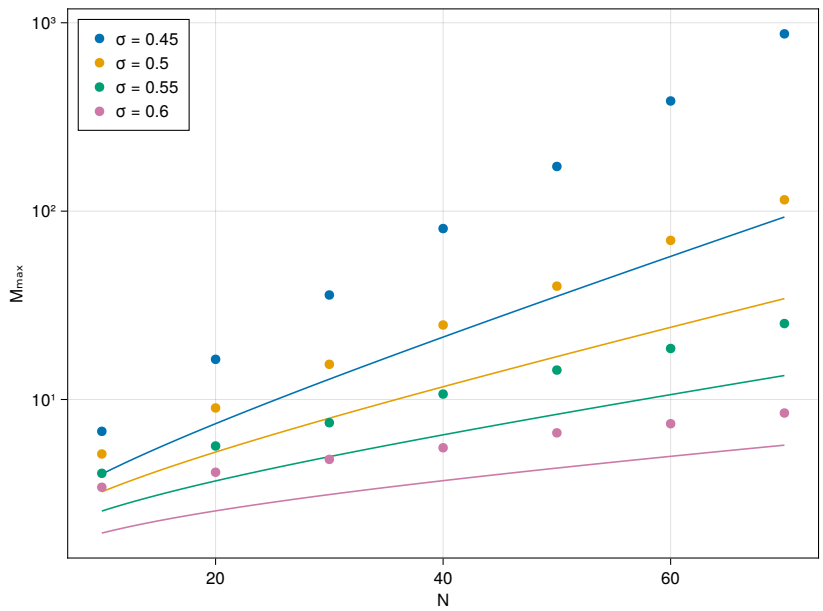

Figure E.1: Plot of the storage capacity of the Exp_β network at $\beta \to \infty$ with normally distributed patterns. Dots represent means ($\pm$ s.e.m.) over 1000 simulations, in which the capacity is determined by the number of patterns sampled until one of the pairwise distances is smaller than $2r$. The standard error is too small to be visible. Lines correspond to the bound in Eq. 80. Note that the plot is log-linear, so the linear increase indicates that $M_{\max}$ scales exponentially in N.

We now parameterize the radius r in terms of the largest tolerable noise amplitude, according to Eq. 71. This gives us

$$M_{\max} = 2\,\text{erfc}\left(\frac{\sqrt{N}(1-2\sigma_{\max}^2)}{2}\right)^{-1/2} . \tag{77}$$

Given that the erfc function can be well approximated using the asymptotic expansion

$$\text{erfc}(x) \approx \frac{e^{-x^2}}{\sqrt{\pi}x}\sum_{n=0}^{\infty}(-1)^n\frac{(2n-1)!!}{(2x^2)^n} \tag{78}$$

for large arguments x, we can obtain a tight lower bound of erfc^{-1} as long as N is large and $\sigma_{\max}^2 \lesssim 1/2$ with the inverse zeroth order expansion, thereby obtaining

$$\text{erfc}(x)^{-1} \geq \sqrt{\pi}xe^{x^2} . \tag{79}$$

We insert Eq. 79 in 77 and finally obtain

$$M_{\max} \geq \sqrt{2\sqrt{\pi N}(1-2\sigma_{\max}^2)}\exp\left[\frac{N(1-2\sigma_{\max}^2)^2}{8}\right] . \tag{80}$$

□

E.3 Patterns on the hypersphere

E.3.1 Storage capacity

Property 8 (Storage capacity: patterns on the hypersphere)**.** *At $\beta \to \infty$, the average maximum number of patterns that the Exp_β network can store and recall without errors is lower-bounded by*

$$M_{\max} \geq \sqrt{\sqrt{8\pi N}(1-2r^2)}\exp\left[\frac{N(1-2r^2)^2}{4}\right] \tag{81}$$

when each pattern is randomly drawn from $\mathbb{S}^{N-1}$.

Proof. We begin by observing that for two random patterns $\boldsymbol{\xi}^i, \boldsymbol{\xi}^j \in \mathbb{S}^{N-1}$, we have

$$\|\boldsymbol{\xi}^\mu - \boldsymbol{\xi}^\nu\|_2^2 = 2(1 - \boldsymbol{\xi}^{\mu\top}\boldsymbol{\xi}^\nu) \ . \tag{82}$$

The probability distribution for the inner product $\omega = \boldsymbol{\xi}^{\mu\top}\boldsymbol{\xi}^\nu$ can be found in [57], and is given by

$$\omega \sim \frac{1}{\sqrt{\pi}} \frac{\Gamma(\frac{N}{2})}{\Gamma(\frac{N-1}{2})} (1-\omega^2)^{\frac{N-3}{2}} \tag{83}$$

which, for large N, can be approximated as

$$\omega \sim \mathcal{N}(0, \frac{1}{N}) \ . \tag{84}$$

We use Eq. 84 in 82 and obtain

$$\Delta^2 \sim \mathcal{N}(2, \frac{4}{N}) \ . \tag{85}$$

The probability of placing a pair of random points on $\mathbb{S}^{N-1}$ with $\Delta^2 \leq 4r^2$ is thus

$$\mathbb{P}(\Delta^2 \leq 4r^2) = \frac{1}{2} \operatorname{erfc}\left(\frac{\sqrt{N}(1-2r^2)}{\sqrt{2}} \right) \ . \tag{86}$$

The average number of samples of Δ^2 one needs to draw before a sample satisfies $\Delta^2 \leq 4r^2$ is given by $\mathbb{P}(\Delta^2 \leq 4r^2)^{-1}$, and the maximum number of patterns that the network, on average, can store, is therefore

$$M_{\max} = 2 \operatorname{erfc}\left(\frac{\sqrt{N}(1-2r^2)}{\sqrt{2}} \right)^{-1/2} \ . \tag{87}$$

We use the lower bound in Eq. 79 in 87 and finally obtain

$$M_{\max} \geq \sqrt{\sqrt{8\pi N}(1-2r^2)} \exp\left[\frac{N(1-2r^2)^2}{4} \right] \ . \tag{88}$$

□

E.4 Bipolar patterns

E.4.1 Noise robustness

Property 9.1 (Robustness to flipped bits)**.** *Assume that we are given a set of unique patterns $\boldsymbol{\xi}^1, \dots, \boldsymbol{\xi}^M \in \{-1,+1\}^N$ with $\min_{\mu,\nu\neq\mu} \|\boldsymbol{\xi}^\mu - \boldsymbol{\xi}^\nu\|_2 > 2r$, and that the Exp$_\beta$ network is initialized in a distorted pattern $\mathbf{s}^{(0)} = \boldsymbol{\xi}^\mu \odot \boldsymbol{\epsilon}$, where $\boldsymbol{\epsilon} \in \{-1,+1\}^N$, with $\mathbb{P}(\epsilon_i = -1) = \rho, \forall i$. Then, at $\beta \to \infty$, the maximum bit-wise error probability $\rho_{\max}$ with which $\boldsymbol{\xi}^\mu$ can be recovered in at least 50% of trials is*

$$\rho_{\max} = r^2/4N \ . \tag{89}$$

Proof. With $\mathbf{s}^{(0)} = \boldsymbol{\xi}^\mu \odot \boldsymbol{\epsilon}$, we have

$$\|\boldsymbol{\xi}^\mu - \mathbf{s}^{(0)}\|_2^2 = \|2\boldsymbol{\epsilon}_{\mathcal{B}}\|_2^2 = 4\|\boldsymbol{\epsilon}_{\mathcal{B}}\|_2^2 \tag{90}$$

where $\boldsymbol{\epsilon}_{\mathcal{B}} \in \{0,1\}^N$, with each entry being a random variable distributed as $(\boldsymbol{\epsilon}_{\mathcal{B}})_i \sim \text{Bernoulli}(\rho)$. This implies that $\|\boldsymbol{\epsilon}_{\mathcal{B}}\|_2^2 \sim \text{Binomial}(N, \rho)$, which can be approximated as $\mathcal{N}(\rho N, \rho(1-\rho)N)$ for large N. This gives

$$4\|\boldsymbol{\epsilon}_{\mathcal{B}}\|_2^2 \sim \mathcal{N}(4\rho N, 16\rho(1-\rho)N) \ . \tag{91}$$

Again, the original pattern $\boldsymbol{\xi}^\mu$ will only be recovered if $r^2 - \|\boldsymbol{\xi}^\mu - \mathbf{s}^{(0)}\|_2^2 \geq 0$, which is satisfied in at least 50% of trials if $r^2 \geq 4\rho N$. The maximum bit-wise error probability with which this type of recovery still holds is thus

$$\rho_{\max} = r^2/4N \ . \tag{92}$$

□

In Eq. 71, σ roughly quantifies the maximum noise fluctuation around a pattern that is tolerable with a given radius r, while still being able to recover the pattern in a majority of trials. In the case of Eq. 92, ρ instead quantifies the maximum tolerable bit-wise error probability.

E.4.2 Storage capacity

Property 9.2 (Storage capacity: bipolar patterns)**.** *At $\beta \to \infty$, the average maximum number of bipolar patterns with sparseness f that the Exp$_\beta$ network can store and recall without errors is lower-bounded by*

$$M_{\max} \geq 2\left(\frac{\pi N}{2\tilde{f}(1-\tilde{f})}\right)^{1/4}\left(\tilde{f}-4\rho_{\max}\right)^{1/2}\exp\left[\frac{N(\tilde{f}-4\rho_{\max})^2}{4\tilde{f}(1-\tilde{f})}\right] \tag{93}$$

where $\tilde{f} = 2f(1-f)$ and $\rho_{\max}$ is the maximum bit-wise error probability tolerated by the network.

Proof. This proof is, again, a slightly modified variant of the proof of Property 7. First, we observe that for two random patterns $\boldsymbol{\xi}^\mu, \boldsymbol{\xi}^\nu \in \{-1,+1\}^N$ with sparseness f, so that $\mathbb{P}(x_i^{\mu,\nu}=1) = f$, it is true that

$$\frac{1}{4}\|\boldsymbol{\xi}^\mu - \boldsymbol{\xi}^\nu\|_2^2 \sim \text{Binomial}(N, \tilde{f}) \tag{94}$$

where $\tilde{f} = 2f(1-f)$ denotes the probability that $\boldsymbol{\xi}^\mu$ and $\boldsymbol{\xi}^\nu$ differ at any given entry. For large N, we can again approximate $\text{Binomial}(N, \tilde{f})$ with $\mathcal{N}(\tilde{f}N, \tilde{f}(1-\tilde{f})N)$, which gives us

$$\|\boldsymbol{\xi}^\mu - \boldsymbol{\xi}^\nu\|_2^2 \sim \mathcal{N}(4\tilde{f}N, 16\tilde{f}(1-\tilde{f})N)\ . \tag{95}$$

We use this to compute the upper bound of the probability of drawing a distance Δ^2 which satisfies $\Delta^2 \leq 4r^2$, as in Eq. 74. The result is

$$\mathbb{P}(\Delta^2 \leq 4r^2) = \frac{1}{2}\,\text{erfc}\left(\frac{\tilde{f}N - r^2}{\sqrt{2\tilde{f}(1-\tilde{f})N}}\right)\ . \tag{96}$$

Following the same derivations used to produce Eqs. 75 and 76, we arrive at

$$M_{\max} = 2\,\text{erfc}\left(\frac{\tilde{f}N - r^2}{\sqrt{2\tilde{f}(1-\tilde{f})N}}\right)^{-1/2}\ . \tag{97}$$

As before, we parameterize the radius r in terms of the maximum tolerable bit-wise error probability according to Eq. 92 and yield

$$M_{\max} = 2\,\text{erfc}\left(\frac{\sqrt{N}(\tilde{f}-4\rho_{\max})}{\sqrt{2\tilde{f}(1-\tilde{f})}}\right)^{-1/2}\ . \tag{98}$$

We finally replace erfc with the lower bound in Eq. 79. This is valid for large N and when $\rho \lesssim \tilde{f}/4$. We obtain

$$M_{\max} \geq 2\left(\frac{\pi N}{2\tilde{f}(1-\tilde{f})}\right)^{1/4}\left(\tilde{f}-4\rho_{\max}\right)^{1/2}\exp\left[\frac{N(\tilde{f}-4\rho_{\max})^2}{4\tilde{f}(1-\tilde{f})}\right]\ . \tag{99}$$

□

E.5 Comparison to the softmax network

To make a illustrative comparison between the softmax and the Exp$_\beta$ network, we plot a set of random patterns on the two-dimensional unit sphere $\mathbb{S}^2$, together with the boundaries of their attractor basins at zero temperature (i.e., $\beta \to \infty$). The result is shown in Fig. E.2. While the basins of the Exp$_\beta$ network form spherical caps around the stored pattern, the basins of the softmax network form Voronoi cells. Since the softmax network parcellates the entire pattern space into a Voronoi diagram, its attractor basins are typically larger than those of the Exp$_\beta$ network. However, it will always converge to one of the stored patterns, regardless of where we initialize the model (assuming it is not precisely on a boundary). In contrast, if the Exp$_\beta$ network is initialized far from all patterns, it will converge to the origin, which can be interpreted as an agnostic state, indicating that the model cannot associate the input query with any of its stored patterns. Finally, as we increase the temperature ($\beta < \infty$), the boundaries of both networks become progressively fuzzier.

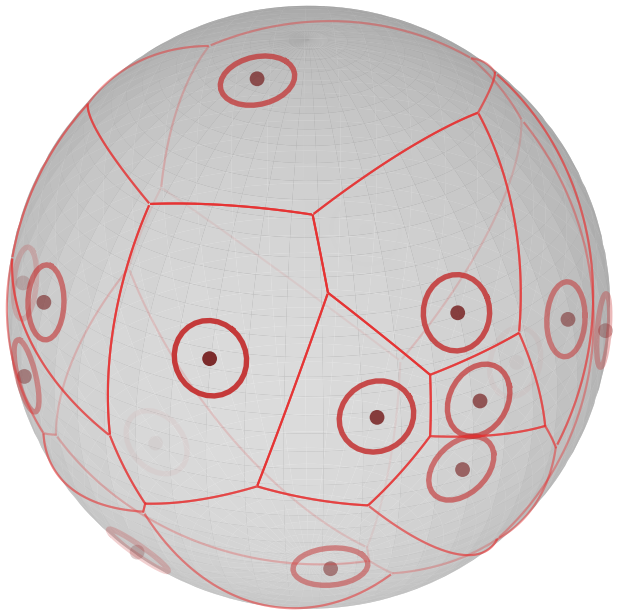

Figure E.2: Plot of patterns on $\mathbb{S}^2$ together with attractor basins at $\beta \to \infty$. Dots represent patterns ($M = 17$) while thick and thin red borders correspond to the boundaries of the attractor basins according to the Exp_β network and the softmax network, respectively. The radius of the circular boundaries has been set to half the minimum pairwise distance between the patterns.

F Comparison to neuron models with active dendrites

To demonstrate how single neurons in kernel attractor networks are generalized models of abstract neurons with active dendrites, we begin by considering a neuron in the feature representation (Eq. 5). We will typically use a Heaviside activation function instead of sgn, and assume patterns and states in $\{0, 1\}^N$, where N is the number of inputs. This, however, does not change the fundamental properties of our model, as SVMs can be formulated for binary data with a minor modification. Assuming a polynomial feature map $\boldsymbol{\phi}$ of degree p, the feature vector will consist of all possible monomials of degree $\leq p$ composed of the states of its input neurons. Setting, for example, $p = 2$ gives us

$$\begin{aligned}\boldsymbol{\phi}(\mathbf{x}) = (&1, \sqrt{2}x_1, \ldots, \sqrt{2}x_N, \\ &\sqrt{2}x_1x_2, \ldots, \sqrt{2}x_1x_N, \sqrt{2}x_2x_3, \ldots, \sqrt{2}x_{N-1}x_N, \\ &x_1^2, \ldots, x_N^2)\ .\end{aligned} \tag{100}$$

By limiting the feature map to only include a subset of all terms, our model is reduced to the 2-degree *sigma-pi unit* [53, p. 73], which can be written as

$$s_{\text{out}} = \Theta\left[\sum_i w_i \prod_{j \in \mathcal{C}_i} s_{\text{in},j}\right] \tag{101}$$

where w_i is the weight of cluster i, which consists of a product of all inputs with indices contained in the set $\mathcal{C}_i$. From a neurophysiological perspective, each product represents the cross-talk between a set of synapses. By including such multiplicative interactions, synapses can both gate and amplify each other, to generate supra-linear input currents. If we now further constrain this model to include only a subset of the cross-terms x_ix_j, $i \neq j$, and parameterize each weight as $w_{ij} = w_iw_j$, our

neuron model is reduced to the *clusteron* [40], which can be written as

$$
\begin{aligned}
s_{\text{out}} &= \Theta\left[\sum_{i}^{N}\sum_{j\in\mathcal{C}_i} w_i w_j s_{\text{in},i} s_{\text{in},j}\right] \\
&= \Theta\left[\sum_{i}^{N} w_i s_{\text{in},i}\left(\sum_{j\in\mathcal{C}_i} w_j s_{\text{in},j}\right)\right]
\end{aligned}
\tag{102}
$$

where $\mathcal{C}_i$ now is the set describing all inputs j that input i should be paired with.

We now consider a neuron in the kernel representation (Eq. 6) with an inner-product kernel $K(\mathbf{x}_i, \mathbf{x}_j) = k(\mathbf{x}_i^\top \mathbf{x}_j)$. By setting $\xi_{\text{out}}^\mu = 1$, $\forall\mu$, and assuming binary inputs, our model is reduced to

$$
s_{\text{out}} = \Theta\left[\sum_{\mu}^{M} \alpha^\mu k\left(\sum_{i}^{N} \xi_{\text{in},i}^\mu s_{\text{in},i}\right)\right] \tag{103}
$$

which is equivalent to the pyramidal cell as a 2-layered neural network, as defined in [48]. According to the original interpretation, this neuron model is comprised of M subunits that are connected to both the inputs and the output. Each subunit μ is characterized by the input weights $\boldsymbol{\xi}_{\text{in}}^\mu$ (which mask some of the inputs), the output weight α^μ (which determines how strongly μ influences the response at the soma), and the activation function k.